Progress Report on the Joint a-Spectroscopy Project of the Wisconsin Department of Natural Resources and the State Laboratory of Hygiene – Radiochemistry Unit.

(November, 22, 2000)

Introduction

In this report, a description of some persisting problems encountered with the methods for the analysis of polonium and thorium is discussed, and a description of the way in which these problems have been solved is presented. The standard operating procedure for the analysis of Po-210 is nearly complete; the standard operating procedure for the analysis of the various thorium nuclides must still be written. A copy of the polonium procedure is given in Appendix A. A summary of all of the current radiochemical data is given in Appendix B.

A model has also been developed for the analysis of the gross alpha data. Although the model is used to analyze gross alpha measurements, it will be demonstrated in the future that the model actually has wider applicability, being applicable, for example, to gamma ray detection systems with cylindrical geometry. A copy of the model is included in Appendix C.

Development of the Method for the Analysis of Polonium 210.

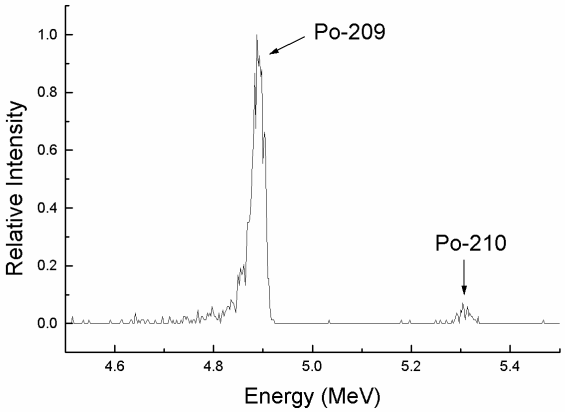

Figure 1. Alpha spectrum with $Pb(NO_3)_2$ reagent.

As mentioned in the previous quarterly report (March 17, 2000), problems were encountered when procedure Po-02-RC (from the Environmental Measurements Laboratory's HASL-300 manual, 28th Ed.) was used to analyze ground water samples for polonium. One problem was that silica gel was forming during the procedure. To prevent the formation of silica gel, when the sample volume had been reduced to about 300 milliliters, the sample was transferred to a 400-mL Teflon beaker and 30 mL of 40% HF was added to the sample. Then the sample was allowed to digest for a period of time in order to convert the ortho-silicic acid of the ground water to fluosilicic acid, thus preventing the formation of silica gel. The present procedure has been updated so that the Teflon beakers are placed in a stainless steel tray filled with water. The water in the tray is brought to a boil on a hotplate, and the water is periodically replenished as needed. Consequently, the sample is digested, and, since the Teflon beaker is in contact with the water of the tray, the sample in the beaker can be evaporated to dryness, thereby getting rid of the excess HF at a temperature which does not lead to excess polonium volatilization. Since the excess HF is vaporized, less boric acid solution is needed to dissolve the insoluble fluoride salts.

Another problem arose when trying to implement the part of procedure Po-02-RC in which the carrier PbS was used to coprecipitate polonium. In the initial step of this part of the procedure the pH of the sample solution is adjusted to a value between 3.5 and 4. However, when the pH was so adjusted in the ground water samples, large amounts of precipitate other than PbS formed in every sample. A portion of this

precipitate was probably composed of insoluble hydroxides like $Mg(OH)_2$ and $Ca(OH)_2$. In addition, when attempts were made to dissolve the precipitate with hydrochloric acid, some of the extraneous precipitate persisted and could only be dissolved by the addition of boric acid. Thus, it seemed that some fluoride precipitate had reformed at the higher pH values, probably due to the reaction of calcium and magnesium with fluoride formed by the following reaction:

$$B(OH)_3F^-(aq) + OH^-(aq) \ ? \ B(OH)_4(aq) + F^-(aq).$$

Since the purpose of the coprecipitation step is to concentrate polonium in the precipitate, while leaving in the supernatant chemical species which might precipitate upon further reduction of the sample volume, it became clear that the PbS coprecipitation step of procedure Po-02-RC was of no value for most of the ground water samples used in this study.

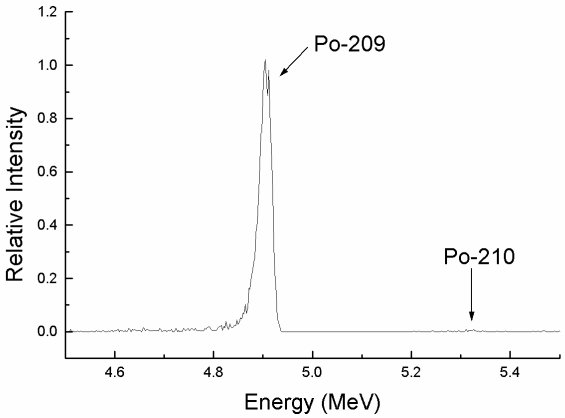

Figure 2. Alpha spectrum without $Pb(NO_3)_2$ reagent.

In addition to the problems encountered during the PbS coprecipitation step, it became evident that much of the Po-210 activity observed in the samples was due to the lead nitrate reagent (Fischer Certified A.C.S.). This is demonstrated by the alpha spectra in Figures 1 and 2. The alpha spectrum in Figure 1 is from a reagent blank (i.e., a sample in which 1 L of deionized water was used instead of ground water) that was prepared using the lead nitrate carrier and performing the PbS coprecipitation step; the alpha spectrum in Figure 2 is from a reagent blank in which the lead nitrate carrier and, consequently, the PbS coprecipitation step were omitted. The same amount of Po-209 tracer was used added to both reagent blanks (67 mBq), and the Po-209 peaks are scaled so that the area of the Po-209 peaks is the same in both spectra. From the spectra it is clear that the lead nitrate reagent is responsible for most of the Po-210 activity. Data from a series of reagent blanks in which lead was added show that the Po-210 activity due to the reagents is about 3.26 mBq with a standard deviation of 0.76 mBq, whereas data from reagent blanks in which no lead was added show that the Po-210 activity due to reagents is about 0.337 mBq with a standard deviation of 0.014 mBq. Since the Po-210 activity for a typical 7-L ground water sample is about 2 to 3 mBq, it is clear that the accuracy of the Po-210 analysis of ground water samples is adversely affected by the addition of the lead carrier.

Since the PbS coprecipitation step proved to be of little value for the ground water samples analyzed so far in this study, and since the lead nitrate reagent introduced much of the Po-210 activity, it was decided that no lead carrier would be added to the samples, and, consequently, that the PbS coprecipitation step would be omitted from the Radiochemistry Units standard operating procedure *SOP ESS RAD Method 008* (see Appendix A). Not using a coprecipitation step in this procedure introduced two problems. First, one sample seemed to have relatively high copper content, so that copper co-deposited with the polonium on the Ni disc during the spontaneous deposition step; consequently, the alpha-spectrum peaks of this sample were broadened by the deposited film of copper. (A PbS coprecipitation step would not remedy this problem since CuS would precipitate under the same conditions as PbS.) Second, some samples contained relatively high levels of sulfate and calcium so that a calcium sulfate precipitate formed when the volume of the sample was reduced. The presence of this precipitate reduced the yield of Po-209 by as much as 50% in a few samples.

A possible solution to the problem of copper deposition would be to try to react the cuprous ion in solution with a ligand or chelating agent, so that the copper complex which would be formed would not deposit on the Ni disc under the conditions used for the spontaneous deposition step. In addition, a perspective ligand

or chelating agent cannot interfere with the deposition of polonium. Library research will be conducted to try to find a ligand or chelating agent with these properties.

Some library research will also be conducted which addresses the problem of the presence of the calcium sulfate precipitate. It would seem that a satisfactory approach would be to chemically alter sulfate to a species that would be soluble in the presence of calcium and magnesium. One such experiment was attempted in which a solution of titanous chloride, $TiCl_2$, was added drop-wise to a calcium sulfate precipitate until the precipitate disappeared. The sulfate was probably reduced to thiosulfate by the following reaction:

$$2CaSO_4(s) + 8Ti^{2+}(aq) + 10H^+(aq) \;?\; 2Ca^{2+}(aq) + 8Ti^{3+}(aq) + S_2O_3^{2-}(aq) + 5H_2O(l).$$

Unfortunately, thiosulfate is unstable with respect to disproportionation. In a warm acidic solution, typical of the conditions used during the spontaneous deposition of polonium, thiosulfate readily disproportionates into elemental sulfur and sulfite. The sulfite then precipitates as calcium sulfite, $CaSO_3$. An alternative approach might be to react the sulfate with some organic reagent to form a sulfate ester which would be soluble in the presence of calcium an magnesium. For example, one might allow the precipitate to react with acetic anhydride:

$$CaSO_4(s) + (CH_3CO)_2O(aq) + H^+(aq) \;?\; Ca^{2+}(aq) + CH_3COOSO_3^-(aq) + CH_3COOH(aq).$$

In summary, in the future some effort will be made to treat the problem of copper deposition on the Ni planchet and to treat the problems encountered in solutions containing high calcium and sulfate levels. In addition, the quality control section of the Po-210 procedure must be finished. The updated standard operating procedure for the analysis of Po-210, *SOP ESS RAD Method 008 Polonium 210*, is given in Appendix A. (For comparison, a copy of Procedure Po-02-RC can be found at web site http://www.eml.doe.gov/publications/procman/ Vol. 1, Sec. 4.54, Procedure Po-RC-02.)

Method for the Analysis of Thorium.

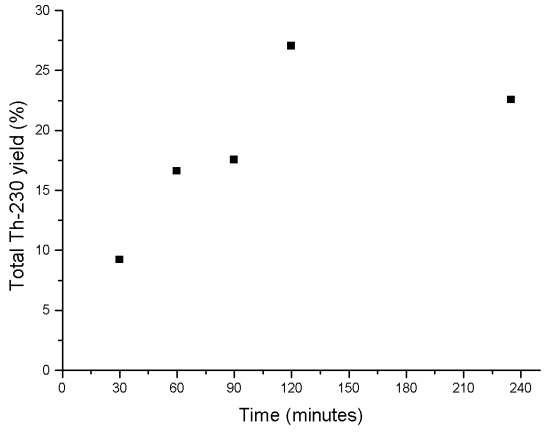

Figure 3. Th-230 yield versus time.

As had been discussed in the previous quarterly report, when Eichrom Procedure ACW10 for the analysis of thorium was implemented, the alpha-spectrum peaks for some of the samples were quite broad, which caused significant overlap between the peaks due to Th-229 and Th-230. As had been discussed, the presence of the broad peaks was not a problem inherent in Procedure ACW10; the problem was readily corrected by assuring that any remnants of the sample in the funnel above the TEVA column were thoroughly removed before the thorium was eluted from the column, thereby assuring that any calcium or magnesium already in or added to the sample would not elute with the thorium. The presence of calcium or magnesium resulted in the formation of the respective fluoride precipitates during the cerium fluoride microprecipitation step. The extra mass due to these precipitates caused the broadening of the alpha-spectrum peaks.

Another problem had been alluded to in the previous quarterly report. It was noted that the overall efficiency or, more properly, the total efficiency of Th-229 in a proficiency sample was only 2.9%. A

possible reason for the low total efficiency was ascribed to the fact that not all of the column operations had been performed promptly, but had been performed over the course of several days. The reasoning was that during this time the column may have dried and developed channels, so that only a small portion of the thorium was eluted. However, when other samples were analyzed, problems with low Th-229 yields persisted. Eichrom Technologies, Inc., the maker of the TEVA column and the supplier for Eichrom procedure ACW10, was contacted in order to inquire about the possible reasons for the low thorium yields and to solicit advice about how to increase the thorium yields. A representative from Eichrom suggested that the problem may be caused by the presence of inorganic phosphate and organic substances which complex thorium causing thorium to moved through the column without binding to the resin. The representative suggested adding some hydrogen peroxide to the samples during a step in which the samples were being digested in concentrated nitric acid, thereby increasing the oxidation potential of the solution and, as a consequence, oxidizing a greater fraction of the organic substances present in the sample. Moreover, the representative suggested using more aluminum nitrate to dissolve the solids which are left after the nitric acid-hydrogen peroxide digestion. The purpose of the aluminum is to bind inorganic phosphate so that the phosphate does not chelate thorium.

Both of the suggestions made by the Eichrom representative were tried, but failed to remedy the problem. Upon making further inquiries, the Eichrom representative revealed that the thorium yields he has gotten using procedure ACW10 have always been quite variable. At this point it seemed that the Eichrom representative could not make any further suggestions that would be of assistance in resolving the problem of low thorium yields in the ground water samples. It was decided that some experiments would be performed for the purpose of determining which step of steps of procedure ACW10 were responsible for the loss of the thorium.

Some experiments were undertaken in order to determine how the conditions used in the cerium-fluoride microprecipitation affected the total yield of thorium. In microprecipitation portion of Eichrom method ACW10 the procedure directs one to allow at least 30 minutes between the time when the HF is added to the centrifuge tube and the time when the cerium fluoride precipitate is filtered. It was decided that in the first set of experiments to be performed that the time allowed between addition of HF and filtration would be varied. The conditions under which the microprecipitation took place were the nearly the same as those used in method Eichrom method ACW10; i.e., 20 mL of 9 M HCl, 5 mL of 6 M HCl, 3.92 pCi of Th-230, and 1 mL of 40% HF were added to a 50-mL centrifuge tube. Figure 3 illustrates the results for a series of such experiments. The figure is of a plot of the percent total yield of Th-230 versus the time between the addition of HF and filtration. From this figure it is quite clear that the Th-230 yield increases quite markedly during the first 2 hours of the microprecipitation. For example, the Th-230 yield after 30 minutes is 9.2 % and that after 2 hours is 27 %, a threefold increase. From the figure it is also noticed that the yield after 4.25 hours decreases, although no attempt has been made to replicate this data point. The reason for the increase of the Th-230 yield during the first two hours is not known. It is possible that, under the prevailing conditions, the cerium fluoride crystals continue to grow and to incorporate thorium during this time period. Another possibility is that the cerium fluoride crystals form relatively rapidly and that, although some thorium may be incorporated into the crystals, some thorium species in solution adsorbs onto the surface of the previously formed crystals. In this case the decline in the Th-230 yield after 4.25 hours may be due to the displacement of the adsorbed thorium species by the adsorption of another species, e.g., fluoride ion. (It should be noted that, as is discuss below, an analogous phenomenon was observed during the coprecipitation of thorium with hydroxyapatite in the presence of fluoride ion.) Whatever the reason is for the time dependence of the Th-230 yield, it became clear that the microprecipitation procedure needed to be altered to maximize the thorium yield. Allowing 2 hours for the microprecipitation to occur was one option, but as is discussed below, such conditions tend to cause the thorium peaks of the alpha spectra to have rather long low-energy tails, a condition that because of their close proximity might tend to cause excessive overlap between the Th-229 and Th-230 peaks. In addition, allowing 2 hours for the microprecipitation, although not totally impractical, is not nearly as convenient as a 30 minute time period.

At this point it was recalled that Canberra, a company which manufactures alpha spectrometers, had a procedure for the preparation of samples for thorium analysis by alpha spectroscopy. The microprecipitation step of the Canberra procedure differed from that of the Eichrom procedure in two ways: (1) instead of using cerium, neodymium was used as the carrier and (2) instead of using 1 mL of HF, 5 mL

of HF was used. It was decided that an experiment would be conducted in which the cerium carrier would still be used but in which 5 mL of HF would be used. The time allowed for the microprecipitation was about 30 minutes. The Th-230 yield in the experiment was 25.5 %, a yield far in excess of the 9.2 % yield obtained when 1 mL of HF was used. Moreover, there was virtually no low-energy tail on the Th-230 peak, in contrast to the previous result in which 1 mL of HF was used and the time allowed for the microprecipitation was 4.25 hours.

Since the use of more HF had such striking results on the Th-230 yield, it was decided that an experiment would be performed in which, in addition to the extra HF, neodymium would be used as the carrier rather than cerium. The resulting Th-230 yield was 30.6 %, an enhancement of about 5 % over the cerium carrier, and, as in the previous case of the cerium, there was virtually no low-energy tail on the Th-230 peak. Consequently, all of the subsequent microprecipitations were performed using 5 mL of HF and using neodymium as the carrier. The modified procedure using the coprecipitation of the Canberra procedure will be referred to as the Eichrom-Canberra procedure.

Table 1. Summary of ground water data.

Well no.	BF210	BF211	BF212	BF210	BF211	BF212
City	Bellevue	Bellevue	Bellevue	Bellevue	Bellevue	Bellevue
Date	3/3/99	6/10/99	6/10/99	3/13/93	3/13/93	3/13/93
Alkalinity (mg/L)	157.00	155.00	148.00	NR	NR	NR
Ba (mg/L)	0.01	0.01	0.02	0.00	0.00	0.00
Ca (mg/L)	129.00	107.00	97.00	NR	NR	NR
Cl (mg/L)	160.00	120.00	120.00	NR	NR	NR
F (mg/L)	1.80	2.00	2.10	2.15	2.35	2.54
Hardness (mg/L)	488.00	413.00	381.00	NR	NR	NR
Fe (mg/L)	0.34	0.29	0.25	NR	NR	NR
Mg (mg/L)	40.00	35.00	34.00	NR	NR	NR
Mn (mg/L)	0.03	0.03	0.03	NR	NR	NR
Ni (mg/L)	0.00	0.00	0.00			
Nitrate (mg/L)	NR	NR	NR	0.25	0.00	0.24
PH	7.50	7.60	7.60	NR	NR	NR
Residue (mg/L)	496.00	828.00	766.00	NR	NR	NR
Sulfate (mg/L)	NR	NR	NR	313.00	216.00	215.00
Na (mg/L)	9.30	79.00	74.00	NR	NR	NR
Zn (mg/L)	0.00	0.01	0.00	NR	NR	NR

NR means that no results were reported for the corresponding analytical parameter.

After implementing the aforementioned modifications for the microprecipitation, it was apparent that the total thorium yield was still quite variable and often very poor. Thus, it became apparent that much of the thorium was being lost in another part of the procedure. In order to be sure that the TEVA columns were working properly, a solution approximating the composition of that which is introduced on the TEVA columns was prepared. On November 9, duplicate solutions were prepared consisting of 0.2 mL of 3.2 M $(NH_4)_2HPO_4$, 0.77 mL of $Ca(NO_3)_2$, 10 mL of 3 M HNO_3-1 M $Al(NO_3)_3$, and 3.92 pCi of Th-230. The solutions were introduced on TEVA columns and processed as directed by the Eichrom-Canberra method. The Th-230 yields for the two samples were 28.1 % and 27.7 %. This result clearly demonstrated that the TEVA columns were working properly and that the low thorium yields were probably the result of little or no thorium coprecipitating with the calcium phosphate carrier used in a previous step of the procedure.

It had been apparent for some time that the thorium yields for two of the quality control samples—the method blank and the laboratory control—were almost always very poor. Moreover, the thorium yields for the most recent batch of ground water samples were consistently higher than the yields for any of the previous samples. For example, a typical result for the yield of the Th-229 tracer (0.747 pCi) added to the samples was 10.2 % in sample no. 78258. This sample had been processed using the microprecipitation procedure in which 1 mL of HF and the cerium carrier had been used; consequently, the 10.2 % yield was quite good. One characteristic which distinguished the most recent batch of samples from previous batches was the relatively high level of dissolved solids. Table 1 gives some results obtained previously by the Wisconsin Department of Natural Resources for the concentrations of various ions in several of the ground water supplies included in the latest batch (This data can be accessed at the Wisconsin Department of Natural Resources web site: http://oraweb.dnr.state.wi.us/inter1/plsql/pws2$.startup.) Consequently, it appeared that one or more constituents in this latest batch of samples had positively affected the efficiency with which the thorium had been coprecipitated by the calcium phosphate precipitate. In order to construct a foundation for the discussion which is to follow, a brief presentation of the properties of the calcium phosphate precipitate and of the chemistry of thorium will be given in the next two paragraphs.

In Eichrom method ACW10 the sample, which has been preacidified with nitric acid (such that pH $\leq$ 2), is reduced in volume by evaporation to between 0.5 and 1 liter. Then, the formation of the calcium phosphate precipitate is brought about by adding 0.2 mL of $(NH_4)_2HPO_4$ solution, 0.5 mL of 1.25 M $Ca(NO_3)_2$ solution, and few drops of phenolphthalein indicator to the sample and adjusting the pH of the warmed sample to the phenolphthalein endpoint with concentrated NH_4OH. The sample is then warmed on a hotplate for about 30 minute. Although Eichrom method ACW10 method states that $Ca_3(PO_4)_2$ is formed during the precipitation, it is highly unlikely that the bulk of the precipitate is composed of $Ca_3(PO_4)_2$. The bulk of the precipitate which forms is more likely to be a nonstoichiometic compound with a composition to very similar to that of hydroxyapatite (HA), which has chemical formula $Ca_{10}(PO_4)_6(OH)_2$. Ions, like fluoride, magnesium, carbonate, are citrate, are readily adsorbed onto the surface of HA.

The discussion of the chemical properties of thorium constitutes a summary of results reported in Gmellin Handbook, Thorium Supplement, Volume D1 (1995). Under the conditions prevailing in all natural waters the +4 oxidation state is the only stable oxidation state of thorium. Because of its relatively high charge and its relatively small ionic radius, 0.984 Å, thorium is a hard Lewis acid. Consequently, thorium has a tendency to only form stable complexes with ligands that are strong Lewis bases, such as fluoride ion and oxygen containing ligands like water, hydroxide ion, and sulfate ion. Moreover, the bonding in these complexes has a high degree ionic character. Other Lewis bases, like chloride, bromide, and iodide, form very weak complexes with thorium. It is thought that the complexes of thorium are characterized by two coordination spheres: an inner sphere composed of molecules of a hard Lewis base or bases and an outer sphere which may contain molecules of either a hard Lewis base like water or a weak Lewis base, or a mixture of the two. In addition, because of the relatively high positive charge density on the thorium ion, thorium tends to form very stable ionic solids, like thorium dioxide, ThO_2, which are highly insoluble in water. In fact, thorium begins undergoing hydrolysis at about pH 2, forming species such as $ThOH^{3+}$ and $Th(OH)_2^{2+}$ and various polynuclear species, and as the pH is increased the extent of soluble hydrolysis products increases until the pH exceeds a value of about 3.5 at which point almost all of the thorium will have precipitated from solution as thorium dioxide. As a consequence, one would expect to find relatively little thorium activity in natural waters. It should be mentioned that prior to these most recent intensive efforts to resolve the problems of poor thorium yields, some experiments were performed in which sodium hydroxide was used to adjust the pH of the solution to bring about the formation of HA. The use of sodium hydroxide allowed higher values of the pH to be attained than could be attained with ammonium hydroxide. It was reasoned that the HA may be acting as a substrate upon which thorium dioxide crystals could be mechanically collected; however, these experiments failed to improve the thorium yields and this approach was abandoned. It is possible that this approach could have worked if the thorium hydroxide was given more time to form, since supersaturation of the hydrolysis products of thorium is a common phenomenon.

Although the concentrations of ions in the most recent batch of ground water samples were relatively high as compared to other ground water samples, the ionic strengths of the samples of the most recent batch were nonetheless somewhat low by many standards, the ionic strengths of the samples being less than 0.01

M. Still, since the ionic strength of the solution affects the chemical activity of thorium, and, therefore, the extent of hydrolysis of thorium, it seemed reasonable to determine whether the ionic strength of the most recent batch of samples could account for some of the increased thorium yield. In the set of experiments described here sodium chloride was used as the electrolyte, although it is not a completely inert electrolyte for these purposes since sodium can be incorporated into the HA lattice and since chloride ion forms weak complexes with thorium. On October 10, samples were prepared by adding 2 mL of concentrated nitric acid and 39.2 pCi of Th-230 to 500 mL of polished water. In addition, enough sodium chloride was added to the samples such that the resulting NaCl concentrations of these samples ranged from 0 M to 6 M. After the HA precipitation step, the HA precipitate was collected on a filter and the alpha-particle activity of the precipitate was measured with a gas proportional counter. Little, if any, activity was detected in these samples, and it was concluded that the ionic strength of the solution probably was not responsible for the thorium yields observed in the latest batch of samples.

Next, it was reasoned that Th^{4+} may not be incorporated into the lattice of HA, but that some complex of thorium, like a sulfate or fluoride complex, may be incorporated into the HA lattice. (It should be noted that the fluoride ion concentration in Table 1 is that for treated waters, so that the actual fluoride concentration in the raw ground water samples may be orders of magnitude lower.) In addition, thorium can form double salts, like $ThSO_4HPO_4$. Consequently, on October 13, a sample was prepared in which 0.4068 g $(NH_4)_2SO_4$, 1 mL of concentrated nitric acid, and 3.92 pCi of Th-230 were added to 500 mL of polished water. The sample was treated as were other samples using the Eichrom-Canberra method; however, there was virtually no thorium yield, and it was concluded that the sulfate probably did not account for the increased thorium yields in the latest batch of samples.

Table 2. Th-230 yield versus amount of fluoride added.

F^- (mg)	Th-230 yield	% Th-230 in ppt.
0.01	0.0	0
0.10	14.7	53
1.1	12.2	44

Another possibility was that the thorium was forming complexes with fluoride ion present in the natural waters, and that the complex was integrated into the HA lattice or that the thorium-fluoride complex was being adsorbed onto the surface of the HA, a plausible possibility since fluoride ion readily adsorbs onto the surface of HA. Consequently, on October 17, three samples were prepared in which 0.01, 0.10, and 1.1 mg of fluoride was added to solutions containing 1 mL of concentrated nitric acid, 3.92 pCi Th-230, and 500 mL of polished water. The samples were run through the Eichrom-Canberra procedure in a single work day. A summary of the results for the Th-230 yield are given in Table 2. This data shows that the addition of small amounts of fluoride lead to significant, albeit somewhat low, yields of Th-230. The fraction of thorium carried with or absorbed to the precipitate, x_p, multiplied by the fraction of thorium which is recovered in the steps following the precipitation, x_r, gives the total yield expressed as fraction, x_T; i.e.,

$$x_p \times x_r = x_T.$$

Immediately after the HA precipitation the precipitate is dissolved then added to the TEVA column. Since the total yield obtained when thorium is added directly to the column is 28 % (form experiments performed on October 9), it is clear that $x_r \approx 0.28$. The values in the third column of Table 2 are $x_p \times 100$, or the percentage of the Th-230 carried with or absorbed to the HA precipitate. Thus, it is seen that at best only about 50 % of the thorium is carried with the precipitate.

On October 18 more experiments were performed in an effort to reproduce the data collected on October 17 and to further characterize the dependence of the thorium yield on the amount of fluoride added to the samples. Six samples were prepared in the same way as those whose results are given in Table 2 except that the amount of fluoride used was 0.02, 0.05, 0.075, 0.1, 1, and 2 mg. When the samples were run through the Eichrom-Canberra method, only the sample containing 0.02 mg of fluoride showed any discernable Th-

230 activity, with the sample having a Th-230 yield of 0.23 %. It should be noted that in this set of experiments, in contrast to the previous set, once the HA precipitate had formed, the precipitates were allowed to sit overnight and the next step in the procedure, which was performed the following morning, was to wash the precipitates with polished water.

Although the results of the previous two sets of experiments using fluoride ion may appear confusing, a relatively simple explanations exists which can account for the two sets of seemingly contradictory data. It has already been concluded that thorium is not incorporated into the HA lattice. Moreover, it is well-known that fluoride readily adsorbs onto the surface of HA. Under the conditions in which HA is formed in this experiment, it is clear that the precipitate is made up of many small HA crystals, so that the precipitate has a relatively large surface area. Furthermore, under these conditions it is clear that the thorium will be in the form of hydrolysis products, fluoride complexes, or some combination of the two. In general, such a complex would have the formula $Th(OH)_xF_y^{4-x-y}$, if polynuclear species are not considered. Such a complex may displace another ion on the surface of HA or, by way of the complexed fluoride, hydrogen bond to some species on the surface of HA. For example, suppose this hypothetical species adsorbs onto the surface of HA displacing ion I,

$$Th(OH)_xF_y^{4-x-y}(aq) + I(HA) \;?\; Th(OH)_xF_y(HA) + I^{z-}(aq),$$

and that this equilibrium is established relatively quickly. Now suppose that the adsorbed thorium species can be displaced by fluoride ion,

$$Th(OH)_xF_y\,(HA) + F^-(aq) \;?\; Th(OH)_xF_y^{4-x-y}(aq) + F(HA),$$

and that this reaction occurs relatively slowly. Then, it is possible for HA to adsorb significant amounts of thorium initially, but if the HA is left in contact with the supernatant for a long enough period of time, the adsorbed thorium species would eventually be displaced by fluoride ion. This could explain why there was very little thorium yield when the precipitate was allowed to sit overnight and washed the next morning. The thorium which by this time had desorbed would be lost with the wash solution. Such a mechanism may explain the microprecipitation data which showed that the thorium yield reached a maximum and then declined with time. However, no attempt has, of yet, been made to reproduce these results.

The previous two sets of experiments showed that the presence of fluoride in the 0.1 to 1.0 mg range can enhance the thorium yield if the HA precipitate is not allowed to be in contact with the supernatant too long. Moreover, although the initial enhancement of the yield due to fluoride was a significant improvement over not having fluoride present, the thorium yields of Table 2 show that under the best circumstances only about 50 % of the thorium was carried with the HA precipitate. It seemed prudent to conduct more research which would lead to a method which would give consistently higher thorium yields and, as a practical matter, would lead to a method in which the precipitate used as the carrier could be left in contact with the supernatant for an indefinite period of time without adversely affecting the thorium yield—sometimes the HA precipitate requires considerable time, many hours, to completely settle to the bottom of the beaker, and because of the large volumes employed during the coprecipitation step (0.5 to 1 L), centrifugation is not practical. It is often convenient to allow the HA to settle overnight, so that the supernatant can be decanted the next day.

Since the presence of the hard Lewis bases in the latest batch of water samples (sulfate and possibly fluoride) could not, by themselves, account for thorium yields obtained, it seemed prudent to conduct some library research on the effect which the various ions found in the ground water samples of the latest batch can have on the chemical properties of HA. A survey of some of the literature on the formation of HA demonstrated that during the precipitation of HA the presence of magnesium can induce the formation of small amounts of crystalline and/or amorphous tribasic calcium phosphate, $Ca_3(PO_4)_2$. Consequently, it was thought that the presence of magnesium in the latest batch of samples may have caused the formation of small amounts of crystalline or amorphous tribasic calcium phosphate, one or either of which may have been the actual phase responsible for coprecipitation of thorium. In order to test this hypothesis and to reproduce the effect of fluoride on the thorium yield, a series of four samples were prepared on October 26.

The samples were prepared by adding the amounts of fluoride, magnesium, and calcium, listed in Table 3 along with 3.92 pCi of Th-230 and 1 mL of concentrated nitric acid to 500 mL of polished water. The samples were subjected to the Eichrom-Canberra method with the exception that no extra calcium was added to the samples.

Table 3. Composition and thorium yields of samples used to test magnesium hypothesis.

Sample no.	F^- (mg)	Mg^{2+} (mg)	Ca^{2+} (mg)	Th-230 yield
1	0	0	40	0
2	1	0	40	0
3	0	40	40	19
4	1	40	40	0

The alpha spectra of samples 1, 2, and 4 were aborted after a few hours since it was apparent that the yield of Th-230 was extremely low or zero. The high Th-230 yield of 19 % for sample 3 shows that the presence of magnesium has a highly beneficial effect on the thorium yield. The result for sample 1 is as expected, the use of HA as the carrier resulted in little or no Th-230 yield. The result for sample 2 was somewhat unexpected in that the presence of about 1 mg of fluoride had in a previous sample resulted in a Th-230 yield of 12.2 %; however, the chemical composition and average crystal size of the HA are probably sensitive to the conditions under which the coprecipitation occurs. Moreover the time in which the precipitate was in contact with the supernatant was not carefully controlled. Sample 4 shows the deleterious effect that fluoride can have on the thorium yield, even when magnesium is present.

At this point it seemed necessary to reproduce and further investigate the positive effect that the addition of magnesium had on the thorium yield. In addition, since fluoride occurs in natural waters and is often added to drinking water supplies, it seemed sensible to investigate ways in which the deleterious effect of fluoride on the thorium yield could be diminished. It was decided that a sample containing calcium, magnesium, and fluoride would be heated in the presence of boric acid, $B(OH)_3$, with the expectation that the boric acid would react with the fluoride. It was anticipated that such a reaction would reduce the concentration of free fluoride thereby diminishing the effect of fluoride on the thorium yield. (It should be mentioned that aluminum in the form of a salt, like $AlCl_3$, can also react with fluoride ion; however, when the pH of the solution is made basic during the HA coprecipitation step, aluminum would precipitate as the hydroxide, $Al(OH)_3$, yielding a gelatinous precipitate which would be difficult to centrifuge and wash.) The samples were prepared by adding the amounts of fluoride, magnesium, and calcium, listed in Table 4 along with 3.92 pCi of Th-230 and 1 mL of concentrated nitric acid to 500 mL of polished water. Samp le 1 was pretreated by adding 5 mL of saturated boric acid solution to sample and warming the sample on a hotplate to near boiling for about 40 minutes. Then the samples were subjected to the Eichrom-Canberra method with the exception that no extra calciumwas added to any of the samples.

Table 4. Composition and thorium yields of samples.

Sample no.	F^- (mg)	Mg^{2+} (mg)	Ca^{2+} (mg)	Th-230 yield
1*	2	40	40	22.0
2	0	40	40	21.3
3	0	80	40	19.4
4	0	80	0	16.9

*Before modified Eichrom method was initiated, 5 mL of saturated boric acid was added to sample and the sample was heated for 40 minutes.

The data in Table 4 show that the positive effect that magnesium had on the thorium yield was reproducible and that the deleterious effect of fluoride could be eliminated by pretreating the sample with boric acid.

Furthermore, the Th-230 result for sample 4 shows that the presence of calcium is not necessary to produce good thorium yield. Under the condition used in the coprecipitation step, it is quite likely that the bulk of the precipitate formed in sample 4 was magnesium ammonium phosphate, $Mg(NH_4)PO_4$. Thus, the possibility exists that the carrier responsible for the high thorium yields is neither crystalline or amorphous tribasic calcium phosphate but magnesium ammonium phosphate. At the present time it is not known whether the lower thorium yield observed for sample 4 is reproducible. If so, then it is likely that another phase, like crystalline or amorphous tribasic calcium phosphate, is responsible for the higher yields in the samples containing calcium. A more thorough investigation of the dependence of the thorium yield on the quantities of magnesium and calcium in the samples will be conducted in the near future.

As of this time many of the ground water samples which had been collected for this project had not been analyzed for thorium, because of the problems previously encountered with the thorium yield. Moreover, it seemed that the major problems encountered with the thorium procedure had been resolved. Consequently, it was decided that these unanalyzed ground water samples would be analyzed for thorium before further method development was initiated. Furthermore, it was decided that 40 milligrams of magnesium would be added to the ground water samples (no calcium would be added because these samples already contained naturally occurring calcium and it was clear that the presence of calcium was not even necessary for good thorium yields) and that 40 milligrams of magnesium and 40 milligrams of calcium would be added to the method blank and the laboratory control, which are included in each batch of samples that are analyzed. This procedure worked quite well with two minor exceptions. First, in a few samples a small amount of gelatinous precipitate formed during the HA coprecipitation step. The gelatinous precipitate was probably calcium and magnesium hydroxide. The presence of the gelatinous precipitate apparently made it difficult to eliminate all of the supernatant from the sample by repeated washing and centrifugation of the precipitate. The HA and gelatinous precipitate were readily dissolved in concentrated nitric acid, but when the resulting solutions were evaporated to dryness, a step used to oxidize any organic compounds still present, a second gelatinous precipitate formed which could not be dissolved by nitric acid solution but was readily digested using 40 % hydrofluoric acid. The second precipitate was, undoubtedly, silica gel which had formed from the ortho-silicic acid originally present in the ground water samples and which had been incompletely removed during the washing of the precipitate composed of HA and the first gelatinous precipitate. The samples which had been digested in hydrofluoric acid readily dissolved in the 3 M HNO_3-1 M $Al(NO_3)_3$ solution used to dissolve the other samples which had been digested in nitric acid prior to introduction on the column. The thorium yields for samples digested in hydrofluoric acid were about 20 %, the same as those in which the silica gel had not formed.

The second problem was encountered with a single sample, sample no. 78255 collected from Winnecone well no. 2. The Th-229 yield for this sample was only 7.6 %. This was the only sample in the study to which polyphosphate had been added at the water treatment facility. Polyphosphate is normally used as a sequestering agent for calcium. Consequently, polyphosphate probably chelates thorium, and if the polyphosphate is not hydrolyzed or otherwise chemically altered, it is conceivable that the chelation of thorium by polyphosphate could keep some of the thorium from coprecipitating and, as a result, reduce the yield of thorium. Thus, it seems probable that the polyphosphate in sample no. 78255 was not completely hydrolyzed when the volume of the sample was initially reduced by evaporation under acidic conditions. Consequently, it may be necessary to alter the procedure so that any polyphosphate that is present is hydrolyzed or chemically altered to a species which does not chelate thorium.

In summary, the thorium yield is significantly increased during the microprecipitation step when the amount of hydrofluoric acid used is increased from 1 milliliter to 5 milliliters. The use of a neodymium carrier during the microprecipitation may result in a better yield than using a cerium carrier, although further experiments should be conducted to reproduce this result. The use of hydrogen peroxide during the nitric acid digestion step does not seem to be necessary for the ground water samples analyzed thus far. Hydroxyapatite is a very poor carrier for thorium; to obtain reasonable thorium yields, it has been demonstrated in the Radiochemistry Unit that magnesium must be either already present in the sample or added to the sample. It is clear that the use of 40 milligrams of magnesium is sufficient to obtain reasonable thorium yields, although more is research is necessary to determine whether the amount of magnesium can be reduced in order that the formation of silica gel in some samples during the nitric acid digestion step be prevented. In addition, careful control of the pH during the HA coprecipitation step may be all that is

necessary to prevent the formation of magnesium and calcium hydroxide. The chemical identity of the actual carrier has not been determined. Magnesium ammonium phosphate probably acts as the carrier when no calcium is present, but either crystalline or amorphous tribasic calcium phosphate may be acting as carriers when calcium is present. If time permits, some effort will be made to try to identify which phase or phases act as carriers. It has been observed that the presence of fluoride often has a detrimental effect on the thorium yield, seemingly by either preventing the thorium from coprecipitating by complexing the thorium or either complexing it or displacing thorium which has adsorbed to the surface of the precipitate. However, it has been demonstrated in the Radiochemistry Unit that when the sample is pretreated using boric acid, the fluoride is chemically bound by the boric acid and does not interfere with the coprecipitation of thorium. It has been observed that the presence of polyphosphate, an agent which probably chelates thorium, has a detrimental effect on the thorium yield. Once again, if time permits, some effort will be made in order to try to find a way of chemically altering the polyphosphate, so that is does not interfere with coprecipitation of thorium. Finally, a standard operating procedure will be written incorporating all of the modifications discussed above.

Analysis of Data for Ground Water Samples.

A preliminary analysis of some of the gross alpha data was performed in preparation for a seminar given in the Water Chemistry Department at the University of Wisconsin-Madison on November 21. A copy of the slides used for the presentation is given in the accompanying PowerPoint file: Water chemistry seminar.ppt. An approximate model used to analyze gross alpha data was developed in this lab. In the gross alpha model the count rate of the alpha-particle detector is related to the activities of the various nuclides that reside in the solid film left in the planchet after the sample has been evaporated. One of the problems of the approximate model was that, in the case of pancake-style gas proportional counters, the alpha particle flux impinging on the detector was overestimated because all of the alpha particles from the sample that traveled a given distance in the direction of the detector were considered to be counted by the detector. In fact, around the outer edges of the detector some of these alpha particles will miss the active region of the detector and not be counted. Originally, it was decided that the contribution of these "edge effects" to the detector signal would be calculated using Monte-Carlo simulations, a method often used in the literature. However, since then, it has proven possible to obtain a formula for the contribution of these edge effects in closed form. The advantages of using such a formula are that some general properties of the solution for the edge effects can be determined which could not be determined using Monte-Carlo simulations, and that one does not need to rely on the use of random number generators or any other possible statistical limitations of the Monte-Carlo method. It should be mentioned that some results for the gross alpha model are purely geometric and can be readily applied to other types of detection systems having cylindrical symmetry. A copy of the model is given in Appendix C. Although not included in the present report, an additional section is being written for the gross alpha model in which the effect of not having a uniform film is examined. Since the effect of the limitations of the gross alpha model used to perform the first data analysis have not been completely characterized, it is advised that the conclusions that are drawn in the presentation of file "Water chemistry seminar.ppt" be considered preliminary.

Conclusions.

Quality control experiments indicate that the methods for the analysis of polonium, uranium, and thorium are working quite well. Some problems still exist for the polonium and thorium procedures which only affect the yield of the tracer in certain samples. In samples with high sulfate concentrations, the yield of the Po-209 tracer has been found to be reduced to about 50% as compared to samples with low sulfate concentrations. It seems likely that the Po-209 yield can be significantly increased by using nitric acid to extract the polonium from the sulfate precipitate. In the case of thorium, the yield of the Th-229 tracer has been found to adversely affected in a single sample. Polyphosphate had been added to this sample before collection. It seems likely that the polyphosphate chelates thorium, keeping thorium in solution during a coprecipitation step. Some effort will be made to determine whether experimental conditions can be altered

in such a way as to assure the hydrolysis of polyphosphate. Finally, a model has been developed for the analysis of gross alpha data. A preliminary analysis of the data was performed for the PowerPoint presentation given in the accompanying file “Water chemistry seminar.ppt.” Since this presentation, the model has been extended to account for the “edge effects” of the detector. In the near future the data will be reanalyzed using this improved model. It should be mentioned that the model can be readily generalized to analyze data in other kinds of measurement systems (e.g., gamma ray detection systems having cylindrical geometry). Moreover, an additional section to the model is currently being written which examines the consequences of not having uniform film.

Appendix A

SOP ESS RAD Method 008 Polonium 210.

Preparation of Water Samples for the Analysis of Po-210.

1.0 Purpose and Applicability.

The purpose of this standard operating procedure is to give a method of preparing water samples for analysis of Po-210 by alpha spectroscopy. This method includes all steps up to but not including the collection of the alpha spectrum, although the calculations used to analyze the alpha spectrum are discussed in this method. This method is applicable to freshwater samples, including tap water, groundwater, and surface waters, which do not contain large amounts of suspended materials. The method may very well be applicable to water samples containing suspended materials and to waters with higher solute concentrations than fresh water, although the method has not as yet been tried with such samples.

2.0 Summary.

Initially, procedure Po-02-RC of the Environmental Measurements Laboratory, United States Department of Energy (Reference 13.1), was used to analyze for Po-210 in tap water samples of the City of Madison. It was found that a gelatinous precipitate formed upon evaporating several liters of the acidified water sample down to a volume of about 100 milliliters (procedure Po-02-RC requires that the volume be reduced to 5 milliliters). Based on the chemical properties of the gel and an analysis of the dried gel by the Inorganics Section of the Wisconsin Occupational Health Laboratory, it was determined that the precipitate was silica gel, which probably had various metal cations bound to it.

Ground water samples can contain up to 14 ppm SiO_2 (Reference 13.4), which ordinarily reacts with water to form silicic acid, $Si(OH)_4$, i.e.,

$$SiO_2(s) + 2H_2O(l) \ ? \quad Si(OH)_4(aq).$$

Strong acids catalyze the polymerization of silicic acid to silica gel (Reference 13.11). Silica gel acts as a cation exchange medium; thus, its presence is unacceptable in any procedure for the analysis of polonium. Once formed, the dissolution of silica gel requires rather extreme conditions—silica gel can be dissolved with hot concentrated hydrofluoric acid (References 13.7, 13.8, and 13.9). However, in this procedure, in order to save time, it seemed prudent to add hydrofluoric acid to the solution prior to the formation of silica gel. The hydrofluoric acid reacts with silicic acid, $Si(OH)_4$, to form fluosilicic acid, H_2SiF_6, a compound that is soluble in water and that does not polymerize, at least not under the conditions used in this method. Thus, in this procedure hydrofluoric acid is added to the acidified sample once the volume of the sample is reduced to 300 milliliters.

After the addition of hydrofluoric acid the volume of the sample is further reduce to about 5 to 10 milliliters. Then, boric acid is added to the sample, and the sample is heated for a period of time in order to dissolve insoluble fluoride precipitates.

Once a clear solution is obtained, polonium is coprecipitated out of solution using a Pb carrier. The precipitate is dissolved in hydrochloric acid, and the polonium is spontaneously deposited from solution onto a Ni disc. Using Po-209 as a tracer, the Po-210 activity can be determined using alpha spectroscopy.

It should be mentioned that the solution chemistry of polonium is not well understood, especially at the tracer level (Reference 13.13). Thus, although an effort is made to outline the relevant chemistry in this procedure, it is not possible to do so unambiguously at every step.

3.0 Interferences.

3.1 **Effect of pH.** During most of the procedure it is important to keep the pH of the solution below a value of about 1. At values of pH above 1 polonium can adsorb onto the walls of the container, causing substantial loss in the amount of polonium. An exception to this is when the pH of the solution is adjusted to about 3.5 to 4 in the centrifuge tubes (step **Error! Reference source not found.**). In a succeeding step the contents of the centrifuge tubes are acidified, which should cause any adsorbed polonium to redissolve. Also, in step 9.7 it is important not to reduce the volume of the solution below five milliliters so that when the solution is subsequently diluted, the pH will remain below 1. (If the level of the solution drops below 5 milliliters, concentrated nitric acid can be added in order to reduce the pH.)

3.2 **Effect of Particulates.** Much experimental evidence suggests that polonium adsorbs on the surface of particulate matter, such as dust, precipitates, and colloids, especially at values of pH exceeding 1. Furthermore, polonium can occur as inclusions in precipitates. Thus, in addition to keeping the pH less that 1, it is important, as much as possible, to exclude dust from the water samples and to ensure that any precipitates that form be completely redissolved. Fluoride precipitates form when the sample is digested with hydrofluoric acid (steps 9.6 and 9.7). [The solubilities of CaF_2 and MgF_2 in cold water are 16 ppm and 76 ppm, respectively (Reference 13.12).] These precipitates are effectively redissolved with boric acid (steps 9.8 to 9.13), although, as is discussed in the next section, care must be taken to ensure that the precipitate is dissolved from the wall of the Teflon beaker. In addition, when the solution to which the boric acid was added cools (step 9.14), boric acid may precipitate owing to the high concentration of solutes and the further concentration of solutes by evaporation. This precipitate is readily dissolved by adding water to the solution.

Another possible interference due to particulates arises during the spontaneous deposition of polonium onto the Ni disc. Any particulates that are present in the solution can settle on the Ni disc causing a reduction in the number of alpha particles reaching the detector and a broadening of the alpha spectrum peaks. Particulates are removed by filtering the solution in step 9.18. In addition, the filter step is necessary because particulates present during the spontaneous deposition of polonium may act as nucleation centers promoting the deposition of polonium on the nuclei rather than the surface of the Ni disc.

.

3.3 **Adherence of Fluoride Precipitates to Teflon.** Some of the fluoride precipitate which forms during the digestion of the sample with hydrofluoric acid (steps 9.6 and 9.7) strongly adhere to the bottom and walls of the Teflon beaker. When the precipitate is redissolved with boric acid, care must be taken to ensure that any precipitate above the level of the solution is redissolved. This can be done by raising the level of the solution in the Teflon beaker to the level of the precipitate with additions of polished water and by scraping the precipitate into solution with a rubber policeman.

3.4 **Polonium Volatilization.** Metallic polonium is quite volatile. At 55 C, 50% of polonium metal is vaporized into the air after a period of 45 hours (Reference 13.12). Although polonium is usually found in solution in the +2 and +4 oxidation states, it is often advised that any kind of sample being analyzed for polonium not be heated while dry. Thus, in step 9.7, in addition to not evaporating all of the acid for the reason discussed in section 3.1, the sample should not be heated to dryness because of possible loss of polonium due to vaporization. An exception to this rule is when the Ni disc, containing the spontaneously deposited polonium, is heated in air (see step 9.26). This is done to oxidize the deposited

metallic polonium in order to lessen its vapor pressure so that the degree to which the polonium contaminates a detector during the collection of an alpha spectrum is diminished (Reference 13.10). Although it may seem that much of the polonium would be lost when the Ni disc is heated, probably less than 10% of the polonium is lost because submonolayer amounts of polonium seem to adhere to the most metal surfaces more strongly than polonium atoms adhere to the surface of polonium metal.

Effect of Oxidizing Species. Because of the half-cell reaction

$$Ni^{2+}(aq) + 2e \; ? \quad Ni(s) \quad E^\circ = -0.23 \text{ V},$$

a Ni disc residing in pure water will tend to have an electrochemical potential of less than –0.23 V versus the standard hydrogen electrode. These conditions would be ideal for the spontaneous deposition of polonium, which has a critical deposition potential of about 0.81 V. (Any potential less than 0.81 V would favor the deposition of polonium.) However, the solution contains oxidizing species, such as O_2, NO_3^-, and Fe^{3+}, which can raise the electrochemical potential of the Ni disc and prevent polonium from depositing or cause the re-oxidation of any polonium which has already deposited on the Ni disc. Adding excess ascorbic acid, a reducing agent, will electrochemically reduce these oxidizing species, thus diminishing their concentrations to acceptable levels, and will lower the electrochemical potential of the Ni disc so that the deposition of polonium is thermodynamically favorable.

Effect of Glassware used for Other Procedures. Po-210 is near the end of the U-238 decay series. Consequently, glassware employed in other procedures that use some of the isotopes of the U-238 decay chain as spikes—e.g., U-238, U-234, Th-230, and Ra-226—can be contaminated with Po-210. Since, under a variety of conditions, polonium strongly adheres to the surfaces of a glass containers, a simple washing will usually not remove all of the Po-210 contamination. Thus, it is important to use proper cleaning procedures to remove all of the Po-210 contamination, or, better still, to isolate glassware intended for Po-210 analysis from other analyses.

Effect of Adding a Lead Carrier. Procedure Po-02-RC (ref. 13.1) calls for the additions of lead nitrate, which is precipitated later in the procedure as PbS, using thioacetamide. In the current procedure a lead carrier is not used because it has been found that the lead adds about 3.3 mBq of Po-210 to the sample, an activity which many times exceeds the activity of the original sample. Moreover, since thioacetamide is not used, there is less hazardous waste to dispose of.

Effect of high sulfate levels. When sulfate and calcium are present at high levels, calcium sulfate, $CaSO_4(s)$, can form when the volume of the solution is reduced by evaporation. It has been observed that the presence of a calcium sulfate precipitate can reduce the yield of polonium by 50%. The polonium may be in the solution which is retained by the precipitate or the polonium may be adsorbed onto the surface of the precipitate. In either case the yield of polonium is reduced. Thus, it is important to prevent the formation of the precipitate or to chemically alter the precipitate to a form which is soluble. It has been observed in the Radiochemistry Unit that the addition of titanous chloride to sulfate containing solutions causes the dissolution of precipitate. $TiCl_2$ is a fairly powerful reducing agent, and the following reaction possibly take place:

$$2CaSO_4(s) + 2Ti^{2+}(aq) + 4H^+(aq) \; ? \quad 2Ca^{2+}(aq) + 2Ti^{3+}(aq) + S_2O_3^{2-}(aq) + 2H_2O(l).$$

Both calcium thiosulfate, CaS_2O_3, and magnesium thiosulfate, MgS_2O_3, are highly soluble. Unfortunately, thiosulfate disproportionates in an acidic environment at temperatures exceeding 60 C by the following reaction:

$$S_2O_3^{2-}(aq) \; ? \quad S(s) + SO_3^{2-}(aq).$$

The bisulfate, SO_3^{2-}, then precipitates with calcium:

$$Ca(aq) + SO_3^{2-}(aq) \;?\; Ca\,SO_3(aq)\,(s),$$

forming an insoluble precipitate. Since thiosulfate is a nucleophile, it may be possible to react thiosulfate with a chemical like methyl iodide, which may be stable at high temperature and high acidity. This must be researched more fully.

Effect of Copper. When cupric ion, Cu^{2+}, is present in solution at high levels, it is possible for copper to electrodeposit on the Ni disc during the spontaneous deposition of polonium. The deposition process is given by the following reactions:

$$\text{Ascorbic acid} \;?\; 2e(Ni) + \text{dehydroascorbic acid},$$

$$Cu^{2+}(aq) + 2e(Ni) \;?\; Cu(Ni).$$

Given that the reduction potential for the reaction,

$$Cu^{2+}(aq) + 2e \;?\; Cu^{\circ} \quad E^{\circ} = -0.23\ V,$$

it is not surprising that copper would electrodeposit on the Ni disc. The deposition of copper on the Ni disc is evidenced by the appearance of a copper colored film on the Ni disc. In addition, the alpha spectra of such discs are broadened, giving supporting evidence that something other than polonium has deposited.

It may be possible to prevent the deposition of copper by complexing the cupric ion in solution. This will be the topic of future research.

4.0 Definitions.

4.1 **analytical batch**: a group of samples which are analyzed together. An analytical batch can include samples from different preparation batches, even samples originating from more than one matrix, and can exceed twenty samples. (modified from the definition due to the NELAC Quality Systems Committee)

4.2 **chemical recovery**: the fraction of the initial amount of the analyte of interest which is present in the last step of sample preparation.

4.3 **contamination**: the difference between the amount of Po-210 activity in a *method blank* (*q.v.*) and the amount of Po-210 activity which is to be expected in the method blank as determined by analyzing a series of *reagent blanks* (*q.v.*). Contamination can occur if some amount of a Po-210 standard has been accidentally introduced into one or more of the reagents or if a new lot of reagents has either significantly more or significantly less Po-210 activity than the previous lot. Notice that when the Po-210 activity of a new lot of reagents differs significantly from the previous lot, the contamination can be either positive or negative. In either case a new series reagent blanks may have to be analyzed to determine the contribution of the new lot of reagents to the Po-210 activity of the prepared sample.

4.4 **detector efficiency**: the ratio of the count rate due to a particular nuclide in a prepared sample, as detected by some instrument, to the total activity of the nuclide present in the prepared sample. The detector efficiency of an instrument is determined by measuring the

count due to a sample with nuclide(s) of known activity, and dividing the result by the known activity:

$$\text{detector efficiency} = \frac{\text{count rate of nuclide(s) as meaured by the instument}}{\text{known activity of the nuclide(s)}}.$$

4.5 **laboratory control sample**: a type of sample prepared by the analyst in which a known amount of Po-210 activity has been added to 1 L of polished water. This sample is analyzed using the same methods as a regular ground water sample. One laboratory control sample must be included in each preparation batch.

4.6 **matrix** (*plural* **matrices**) –the component or substrate that contains the analyte of interest. In the case of the current analytical method, the matrix is groundwater. In the future this analytical method may be extended to other matrices.

4.7 **analytical method**: the procedure for the determination of the concentration or activity of a particular analyte. The analytical method may be divided into several parts: (1) collection of the sample, (2) pretreatment of the sample (e.g., the acidification of the sample in the field), (3) preparation of the sample (e.g., extraction, digestion, concentration, or some combination of these) for analysis, (4) collection of raw data for a the sample with a given instrument, and (5) calculations involved in reducing the raw data to an analyte concentration or activity.

4.8 **method blank**: a sample in each preparation batch that is prepared in the same way as a reagent blank but is analyzed in exactly the same way as the other samples. Thus, ideally, the net concentration or activity of the analyte of interest in the method blank is zero. However, in general, the method blank is expected to deviate a small amount either positively or negatively from zero. Criteria for determining whether this deviation is acceptable are given in the *Quality Control* section.

4.9 **method detection limit**: the minimum concentration of the analyte that can be measured and reported with 99% confidence that the analyte concentration is greater than zero and is determined from analysis of a sample in a given matrix containing the analyte (40 CFR Part 136, Appendix B).

4.10 **polished water**: (incomplete).

4.11 **preparation batch**: a group of one to twenty environmental samples of the same NELAC-defined matrix which are made ready for analysis with the same process or processes and by the same personnel, using the same lot(s) of reagents, with a maximum time of twenty-four hours between the start of processing of the first sample and the start of processing of the last sample.

4.12 **prepared**: an adjective used to describe a sample which has been subjected to the analytical method up to but not including the sample analysis.

4.13 **proficiency test sample**: a type of sample from an entity that is separate from the laboratory of interest and which has a concentration known only to the outside entity.

4.14 **reagent activity**: the activity, above background, of the analyte of interest in a reagent blank.

4.15 **reagent blank**: a 1 liter sample of polished water that is prepared for analysis in the same way that a normal sample of ground water is prepared for analysis, with the exception that a Po-210 spike is never added to the polished water sample. (If a groundwater sample is 10 liters and has been pre-acidified with 10 milliliters of concentrated nitric acid, then 10 milliliters of concentrated nitric acid must be added to the 1 liter of polished water.)

4.16 **replicates**: two or more subsamples that are equal portions of the same sample. A pair of replicates must be included with each preparation batch.

4.17 **sample**: the collection of matter that is to be subjected to the analytical method. In the case of the current analytical method, it is a certain volume of groundwater; a laboratory control sample, a method blank, or a proficiency sample.

4.18 **subsample**: a representative portion of a sample that is subjected to the analytical method.

4.19 **sample analysis**: both the procedure whereby raw data for a particular prepared sample is collected using some instrument or instruments (in this procedure an alpha spectrometer) and the calculations that are involved in reducing the raw data into an analyte concentration or activity.

4.20 **sample preparation**: the steps following the collection of the sample and preceding the analysis of the sample. These steps include any pretreatment of the sample (e.g., acidification with nitric acid in the field) and the chemical and physical processes involved in readying the sample for analysis.

4.21 **total efficiency**: the total number of alpha-particle counts of a particular nuclide that are detected with the alpha spectrometer in a given time interval divided by the known activity of the tracer added to the sample and the time interval:

$$\text{total efficiency} = \frac{\text{total number of alpha particle counts detecetedin a given time interval}}{\text{known activity of tracer added to the sample} \times \text{time interval}}.$$

The overall efficiency is the product of the chemical recovery and the detector efficiency:

$$\text{total efficiency} = \text{chemical recovery} \times \text{detector efficiency}.$$

4.22 **tracer**: a nuclide which is an isotope of the analyte of interest, so that nuclide has the nearly same chemical behavior as the analyte of interest. Normally, a known activity of the tracer is added to the sample during the preparation stage, and the number of counts of the tracer over a given time period is used to determine the chemical recovery of the tracer which is assumed to be identical to the chemical recovery of the analyte of interest (see chemical recovery, detector efficiency, and overall efficiency).

5.0 Equipment.

5.1 Calcium gluconate gel (Pharmascience).

5.2 Long rubber gloves (about 13½ inches).

5.3 4-L glass beaker (or larger).

5.4 150-mL glass beaker.

5.5 250-mL glass beaker.

5.6 400-mL Teflon beaker.

5.7 1-L graduated cylinder.

5.8 10-mL polymethylpentene graduated cylinder.

5.9 Three 50-mL centrifuge tubes.

5.10 Large Teflon stir bar.

5.11 60-mL polypropylene bottle.

5.12 Glass stir rod.

5.13 Small Teflon stir bar—for use in the deposition cell. Since the Ni disc of the deposition cell is magnetic, stir bars tends to stick to the disc. In order to prevent this a short, stout stir bar is needed. A Fisherbrand 5/16 x 5/8? octagonal magnetic stir bar works.

5.14 Silicone rubber septum (= 0.125 inch thick and = 18 mm in diameter.)

5.15 Rubber policeman.

5.16 Large hotplate.

5.17 Combination hotplate and stirrer.

5.18 Vortex mixer.

5.19 Polypropylene forceps.

5.20 Funnel.

5.21 Whatman No. 41 filter paper.

5.22 100 ^{o}C thermometer.

5.23 360 ^{o}C thermometer.

5.24 1 inch diameter nickel disc.

5.25 Small ointment tin.

6.0 Reagents.

6.1 Polished water.

6.2 Concentrated nitric acid (Fisher Scientific, 68–71%, trace metal grade).

6.3 Concentrated hydrofluoric acid (Fisher Scientific, 47–51%, trace metal grade).

6.4 Concentrated hydrochloric acid (Fisher Scientific, 35–38%, trace metal grade).

6.5 0.5 M HCl—to prepare 1 liter of solution, add 42 mL of concentrated, trace-metal-grade HCl to a 1-L container and add enough polished water to bring the solution volume to 1 liter.

6.6 Boric acid solution (Mallincroft, granular, analytical reagent): 25 g in 500 mL of polished water.

6.7 Standardized Po-209 solution.

6.8 Standardized Po-210 solution.

6.9 L-Ascorbic acid (Fisher Scientific, Certified A.C.S.).

7.0 Related Documents.

ESS RAD GENOP 023 SOP HF—This standard operating procedure describes safety precautions which must be followed when using hydrofluoric acid and procedures to be followed in the event that hydrofluoric acid accidentally comes into contact with one's skin or is accidentally spilled.

8.0 Sample Collection, Preservation, Shipment, and Storage.

8.1 Empty a glass vial containing 40 mL of 8 M nitric acid (1:1 polished water to concentrated nitric acid) into a 20-L polyethylene cubitainer.

8.2 Allow the water tap to run for at least a few minutes.

8.3 Fill the cubitainer about one-half full with the groundwater sample. Shake the solution in the cubitainer in order to mix the acid and groundwater.

8.4 Add groundwater to the cubitainer until the cubitainer is about nine-tenths full. Shake the solution in the cubitainer.

8.5 Add groundwater to the cubitainer until the cubitainer is nearly full. Leave enough air in the cubitainer so that the solution can be mixed. Shake the solution in the cubitainer.

9.0 Procedure.

Introduction.

Each set of samples that are prepared to be analyzed is called a preparation batch. Each preparation batch must contain a replicate of one of the samples, a laboratory control, and a method blank. For more information about these concepts see Section 4.0 *Definitions* and Section 11.0 *Quality Control*. For the sake of clarity the following procedure is written for a single sample, although it is understood that multiple samples are being prepared simultaneously.

Reduction of Sample Volume.

9.1 Transfer a 2.5 L aliquot of the pre-acidified (pH ~ 2) groundwater sample to a 4-L beaker.

9.2 Add 50 mL of concentrated HNO_3, 30 to 80 mBq of Po-209 tracer, and for the laboratory control sample, 30 to 80 mBq of Po-210.

9.3 Evaporate the solution on a hotplate, adding aliquots of the original sample until the desired amount of sample has been added to the 4-L beaker. (A total sample volume of up to 10 liters may be used.)

> It should be mentioned that the groundwater sample should be placed in a single beaker rather than be distributed among several beakers in an attempt to accelerate the evaporation process. The reason for this is that the polonium with adsorb onto the surface of the beakers when the value of the pH is above about 1. Distributing the solution among several beakers may dilute the acid to the point where adsorption occurs. It may be argued that one could just add more nitric acid to the other beakers, but, as is discussed in step 9.6, acid catalyzes the formation of silica gel from solutions which contain silicic acid, such as groundwater. Thus, in such cases it is best to use the least possible amount of nitric acid.

9.4 Evaporate the solution down to a volume of 300 mL.

Digestion of Silicic Acid with Hydrofluoric Acid.

Warning! The use of long rubber gloves is mandatory when handling HF or any solution containing HF. HF can move through the skin rapidly and can cause the precipitation Ca, in the form of CaF_2, in the body tissues. This can lead to necrosis of the affected tissues, even bones. If tissues come in contact with HF, it is important to wash the affected area with copious amounts of water, and to apply calcium gluconate gel to the affected area. A tube calcium gluconate gel is stored in the same cabinet as the hydrofluoric acid. The procedure to be employed if one is exposed to hydrofluoric acid is given in *SOP ESS RAD GENOP 023*.

9.5 Transfer the solution from the 4-L beaker to a 400-mL Teflon beaker. Rinse the 4-L beaker three times with approximately 10 mL portions of polished water, and transfer the rinses to the Teflon beaker.

9.6 Add 30 mL of 40% hydrofluoric acid to the Teflon beaker using a 10-mL polymethylpentene graduated cylinder.

If the hydrofluoric acid is not added to the solution, silicic acid, $Si(OH)_4$, will polymerize by a condensation reaction forming siloxane bonds between adjacent Si atoms; e.g., two silicic acid molecules will undergo the reaction:

$$2Si(OH)_4(aq) \;?\; (OH)_3Si–O–Si(OH)_3(aq) + H_2O(l).$$

This condensation reaction is catalyzed by strong acids. Eventually the silicic acid will polymerize to form colloids, and, then, a gel. The formation of a silica gel will interfere with the analysis of polonium. Firstly, the silica gel acts as a cation exchange medium, and may bind polonium ions. Secondly, the water retained by the silica gel undoubtedly contains polonium ions which, during the spontaneous deposition of polonium on the Ni disc, will only be transferred to the surface of the Ni disc very slowly, thus decreasing the yield of polonium in the procedure.

The hydrofluoric acid reacts with silicic acid to form fluosilicic acid:

$$Si(OH)_4(aq) + 6HF(aq) \;?\; H_2SiF_6(aq) + 4H_2O(l).$$

The fluosilicic acid thus formed is highly soluble in water and will not polymerize.

9.7 Evaporate the solution in the Teflon beaker on a hotplate until the volume has been reduced to about 10 mL. (At the lower volumes white fumes should be observed. Avoid any contact with the white fumes since they contain HF.)

During this step of the procedure it may be noticed that the solution turns an orange-brown color. As the solution is evaporated, both the acidity and the concentration of nitrate in solution increase. As is discussed in step 9.17, nitrate, NO_3^-, functions as an oxidizing agent in acidic media forming nitric oxide, NO. Nitric oxide further reacts with oxygen to form nitrogen dioxide, NO_2, an orange-brown gas which responsible for the color of the solution. As an example, iron in solution in the form Fe^{2+} is readily oxidized to Fe^{3+}, especially under the conditions of high acidity and nitrate concentration which prevail in this solution.

9.8 Place the Teflon beaker in a hot-water bath consisting of a stainless steel pan filled approximately half full with reverse-osmosis (RO) water (see Figure 1), and allow the solution in the beaker to evaporate to dryness.

Warning! During this step some of the HF from the solution in the Teflon beaker may become dissolved in the water of the stainless steel pan. Upon conclusion of this part of the procedure, the pH of this water should be tested, and if the water is sufficiently acidic (pH < 4), the water should be treated as an other kind of HF waste is treated.

Dissolution of Fluoride Precipitates with Boric Acid.

9.9 Add 60 mL of boric acid solution and 40 mL of 0.5 M HCl solution to the Teflon beaker, and place the beaker on a hotplate.

9.10 If precipitates can be seen on the sides of the Teflon beaker, fill the beaker with polished water to a level above that of the precipitates, and use a rubber policeman to scrape the precipitate off the walls of the beaker and into solution. (Since both the Teflon beaker and the precipitate are white, it is often difficult to discern whether there is a precipitate on the walls of the beaker, especially when the beaker contains a solution. Shining a light, such as a flashlight, on the inside wall of the beaker helps to illuminate the areas where precipitate

is adhering.) When adding the polished water, it is a good idea to use a wash bottle to rinse the drops of acid that collect on the sides of beaker back down into solution. Some of these droplets may form on the rim of the beaker and may not be accessible to the stream of water from the wash bottle. Since these droplets contain concentrated HF, it is a good idea to wipe the droplets off of the rim with a paper towel (while wearing rubber gloves, of course), and to allow the towel dry in the hood before discarding it.

The fluoride ions combine with various metal ions in solution to form precipitates, e.g., calcium fluoride, CaF_2, magnesium fluoride, MgF_2, ferric fluoride, FeF_3, and ferrous fluoride, FeF_2. The last two precipitates are green and may impart a green tint to the mixture of fluoride precipitates. Boric acid, $B(OH)_3$, acts as a Lewis acid by complexing fluoride ions which leads to the dissolution of the precipitates; e.g.,

$$CaF_2(s) + 2B(OH)_3(aq) \; ? \quad Ca^{2+}(aq) + 2[BF(OH)_3]^-(aq).$$

In addition, boric acid reacts with excess fluoride ions in solution, greatly reducing the danger posed by hydrofluoric acid.

The solubility of tracer level polonium is not affected when hydrofluoric acid is added to solutions containing hydrochloric acid or sulfuric acid (Reference 13.5). Little or no work seems to have been done on the effect of hydrofluoric acid on nitric acid solutions containing tracer level polonium.

It should be mentioned that aluminum chloride, or some other aluminum salt, may be used, instead of boric acid, to dissolve the fluoride precipitate.

9.11 Turn the hotplate on fairly low so that evaporation is minimal. Allow the solution to warm on the hotplate and to stir for at least 1 hour (this will give the solution time to dissolve the precipitate from the beaker walls). Once the precipitate has dissolved from the walls of the Teflon beaker, increase the heat setting on the hotplate, and allow the solution to evaporate down to about 40 mL. (Once the solution has been reduced , the walls of the beaker should be rinsed with polished water once more to wash any residual HF into solution.)

Although the solution can remove the bulk of the precipitate from the bottom and walls of the Teflon beaker in a relatively short time, much of the precipitate remains suspended in solution in particulate form for some time. Warming the solution accelerates the dissolution process, but complete dissolution may take more than one hour and may require additional aliquots of boric acid solution. In addition, sulfate precipitate may be present, in which case an insoluble calcium sulfate precipitate may form which will not dissolve in boric acid solution.

9.12 Pour a few milliliters of the solution from the Teflon beaker into a 50-mL centrifuge tube. Note whether the solution is clear or turbid. If the solution is clear, go to step 9.14. If not transfer the contents of the centrifuge tube back into the Teflon beaker, and go to the next step.

9.13 Add 5 mL of boric acid solution to the Teflon beaker; then, allow the beaker to warm on a hotplate for about 30 minutes. Repeat step 9.12. Do not use more than 70 mL of the boric acid solution. Any precipitate which persists may be calcium sulfate.

9.14 Transfer the rest of the solution in the Teflon beaker to the 50-mL centrifuge tube. Rinse the Teflon beaker with approximately 5 milliliters of polished water, and transfer the rinse to the centrifuge tube. As the solution cools, a precipitate may form in the centrifuge tube. This precipitate is boric acid and can be dissolved by heating the solution in a water bath before it is transferred to the deposition cell.

Preparation of the Nickel Disc for Spontaneous Deposition of Polonium.

9.15 Using a polypropylene forceps to hold the Ni disc, rinse the nickel disc with ethanol, followed by a rinse with polished water. Then, dip the disc in concentrated HCl for about 2 minutes, again followed by a rinse with polished water.

Preparation of the Hot-Water Bath.

9.16 Prepare a hot-water bath by placing a 400-mL beaker on a combination hotplate and magnetic stirrer and partially filling the beaker with about 200 mL of water. Place a thermometer in the beaker, and adjust the hotplate so that the temperature of the water is maintained at about 80 C.

Preparation of Deposition Cell and Spontaneous Deposition of Polonium.

9.17 Add 100 mg of ascorbic acid and a small stir bar to a 60-mL wide-mouth polypropylene bottle. (A stir bar that is almost round should be used. If a long, narrow stir bar is used, then, because nickel is magnetic, the stir bar will stick to the Ni disc and will not rotate.)

From experiments performed in the Radiochemistry Unit it is clear that uranium, thorium, and actinium do not spontaneously deposit along with polonium on a Ni disc; thus, the common actinides will not give rise to interfering peaks in an alpha spectrum of polonium.

The critical deposition potential for the electrodeposition of poloniumon a Ni disc is about 0.81 V (Reference 13.6), so that polonium will spontaneously deposit on the electrode when the potential of the electrode is less than 0.81 V (versus the standard hydrogen electrode). There are a number of oxidizing species present in the solution which may elevate the potential of the Ni disc to the point that polonium deposition is prevented or that some of the deposited polonium may be re-oxidized. One such species is nitrate, NO_3^-, which has the corresponding half-cell reaction

$$NO_3^-(aq) + 4H_3O^+(aq) + 3e \; ? \quad NO(aq) + 6H_2O(l) \quad E^\circ = 0.96 \text{ V}.$$

It is seen that nitrate is a reasonably strong oxidizing agent in acidic solutions; however, in step 9.10, when the solution is evaporated to dryness, much of the nitrate evaporates as HNO_3, although some nonvolatile nitrate salts could be left behind.

Another potential oxidizing agent is Fe^{3+} which has the correspond half-cell reaction:

$$Fe^{3+}(aq) + 3e \; ? \quad Fe^{2+}(aq) \quad E^\circ = 0.770 \text{ V}.$$

The redox behavior of oxygen is complex, but two reactions of oxygen that can occur in acidic solution are

$$O_2(aq) + 2H_3O^+(aq) + 2e \; ? \quad H_2O_2(aq) + 2H_2O(l) \quad E^\circ = 0.682 \text{ V},$$

$$O_2(aq) + 4H_3O^+(aq) + 4e \; ? \quad 6H_2O(l) \quad E^\circ = 1.229 \text{ V}.$$

Thus, oxygen is capable of raising the potential of the Ni disc, and, therefore may inhibit the deposition of polonium or cause the re-oxidation of any polonium deposited on the Ni disc. Depending on the redox potential of the solution, polonium should be in the +2 or +4 oxidation state or a mixture of the two. During the spontaneous deposition step polonium is in a 0.5 M HCl solution and most of the polonium is thought to exist as anionic chloropolonium complexes like in $[PoCl_3]^-$

and $[PoCl_4]^{2-}$ for the +2 oxidation state and in $[PoCl_5]^{-}$ and $[PoCl_6]^{2+}$ for the +4 oxidation state (References 13.1 and 13.13, pg. 343). In the presence of oxygen, the potential of the Ni disc may exceed 0.81, leading to the oxidation and loss of polonium on the Ni disc. For example,

$$2Po(Ni) + O_2(aq) + 8Cl^-(aq) + 4H_3O^+(aq) \; ? \quad 2[PoCl_4]^{2-}(aq) + 6H_2O(l).$$

Ascorbic acid participates in the following half-cell reaction:

$$\underset{\text{(dehydroascorbic acid)}}{C_6H_6O_6(aq)} + 2\,H_3O^+(aq) + 2e \; ? \quad \underset{\text{(ascorbic acid)}}{C_6H_8O_6(aq)} + 2H_2O(l) \qquad E^\circ = 0.080 \text{ V}.$$

When an excessive amount of ascorbic acid is added to the solution, it can reduce O_2, and any Fe^{3+} or NO_3^- left in solution, and will establish the potential of the Ni disc at about 0.080 V or below, far below 0.81 V, the critical deposition potential of polonium. Consequently, polonium spontaneously deposits on the Ni disc.

It should be noted that, thermodynamically, it is possible for the ascorbic acid to react directly with polonium in solution. However, the rate of this reaction is apparently very slow, possibly because the formation of any polonium apart from the Ni surface would require that the polonium go through a nucleation stage. Typically, there is a high free-energy barrier to the formation of a bulk material formed by nucleation processes because of the high surface area to volume ratio of the nucleation centers. The Ni disc acts somewhat like a catalyst, by transferring electrons from ascorbic acid to Po^{2+}, and Ni acts as a relatively low-energy surface for the deposition of polonium.

9.18 Using a funnel and Whatman No. 41 filter paper, filter the solution from the centrifuge tube into the 60-mL polypropylene bottle (see Figure 2).

The filter step is important in order that any particulate matter that may be present be removed. The particulate matter could act as nucleation centers for the deposition of polonium. Moreover, the particulate matter could settle on the nickel disc, causing a reduction in the alpha-particle signal and a broadening in the peaks of the alpha-particle spectrum.

9.19 Add 10 mL of 0.5 M HCl to the empty centrifuge tube from the previous step, and place the tube in a hot water bath. Once the 0.5 M HCL solution becomes hot, wash the filter with the HCl solution. Discard the filter.

9.20 Place a silicone rubber septum and the clean nickel disc in the cap of the 60-mL bottle, and screw the cap onto the bottle (see Figure 3. (The septum assures that the Ni disc is firmly and squarely seated on the lip of the bottle, thus helping to prevent leakage.)

9.21 Invert the bottle, use a felt tip pen to mark the level of the solution in the bottle (in order that the bottle may be periodically checked for leakage), and pierce a small hole in the center of the bottom of the bottle with a hot glass stir rod (so that when the bottle is heated, as in the next step, the increase in gas pressure above the solution will not force the solution out of the bottle).

9.22 Place the inverted bottle in the hot-water bath (see Figure 4. Turn the magnetic stirrer on, and make sure that the stir bar is spinning. During the first 5 minutes that the bottle is in the hot water bath, remove the bottle several times and tighten its cap to prevent leakage which commonly occurs as a result of the thermal expansion of the polypropylene bottle. Maintain the temperature of the bath at 80 C while stirring for 4 hours. (If the level of the solution in the bottle drops significantly during the four hours, the liquid is probably leaking from the bottle, and the cap on the bottle should be further tightened to prevent excessive leakage. Evaporation should not cause the level of the solution in the bottle to drop significantly.)

9.23 During the deposition process water should be added to the hot-water bath to keep the water near its original level.

9.24 After the four-hour deposition is complete pour the solution from the deposition cell into a bottle designated for acidic waste.

Holding a piece of Parafilm over the hole in the bottom of the bottle with a finger prevents leakage of solution from the hole when the cell is turned upright and the bottle cap is removed.

9.25 Remove the Ni disc, rinse it with polished water and, then, ethanol.

Some corrosion of the Ni disc by the hot acid is normal, and is of no concern.

9.26 Place the Ni disc on a hotplate preheated to 300 C, cover the disc with a 400-mL glass beaker, and leave the Ni disc on the hotplate for 5 minutes.

The purpose of this step is not so much to dry the disc as it is to oxidize the polonium on the surface of the Ni disc. Elemental polonium is quite volatile. The oxidation of polonium lowers the volatility of polonium which significantly reduces the contamination of detectors by polonium. The hotplate to be used for oxidizing the polonium should be prepared before the Ni disc is placed on it. This is done by placing a 400-mL beaker upside down on the hotplate and sliding the end of a thermometer underneath the beaker so that the bulb of the thermometer is in the center of the hotplate. The other end of the thermometer can be supported with another beaker or some other support (see Figure 5. Once the temperature has stabilized at about 300 C, the thermometer can be removed, and the Ni disc can be placed under the beaker for a period of five minutes. A Corning hotplate set at about 6¾ gives a stable temperature of about 300 C. When oxidation has occurred, there should be a noticeable color change in the portion of the Ni disc exposed to the solution during deposition. For example, after oxidation, a Ni disc often has a golden patina. Discs with excessive corrosion often turn black. If there is no color change, increase the temperature of the hotplate, and leave the Ni disc on the plate until such a color change is observed.

9.27 Place the Ni disc in a labeled ointment tin until it is time to collect the alpha spectrum.

10.0 Calculations.

Calculations When the Alpha-Particle Peaks of Po-209 and 210 are Well-Separated.

When the peaks due to Po-209 and Po-210 are well-separated, one can just define two regions of interest (ROI), i.e., two energy intervals, such that one ROI encompasses the Po-209 peak, call it ROI_2, and the other ROI encompasses the Po-210 peak, call it ROI_3 (the notation used for the various regions of interest is further explained in Appendix A). The first parameter that must be calculated it the total efficiency. The total efficiency, $?_O$, is calculated using the following equation:

$$q_O = \frac{N_{2,S} - N_{2,B}\left(\frac{T_S}{T_B}\right)}{A_{209}\, T_S},$$

where $N_{2,S}$ is the number of counts in interval ROI_2, i.e., the number of counts due to Po-209, $N_{2,B}$ is the number of counts in interval ROI_2 of the background spectrum, T_S is the live time of the sample spectrum, T_B is the live time of the background spectrum, and A_{209} is the

activity of the Po-209 tracer added to the sample. The second term in the numerator of the above equation is just the number of counts due to background activity; thus, the numerator is the number of counts in ROI_2 due to Po-209.

The next parameter that must be calculated is the tracer recovery, $?_T$, which is given by

$$q_T = \frac{q_O}{q_D},$$

where $?_D$ is the detector efficiency. The detector efficiency must be determined for each detector. (An SOP is in the process of being written which gives instructions on how to calibrate the detectors). The detector efficiency is typically 40 to 43%.

Next, the activity of Po-210, A_{210}, is calculated using the following formula:

$$A_{210} = \frac{N_{3,S} - N_{3,B}\left(\frac{T_S}{N_B}\right)}{q_O\, T_S} - A_{210,R},.$$

where $N_{3,S}$ is the number of counts in interval ROI_3 of the sample spectrum, i.e., the number of counts due to Po-210, $N_{3,B}$ is the number of counts in interval ROI_3 of the background spectrum, and A_R is the Po-210 activity due to the reagents. It should be mentioned that for a method blank is run with every preparation batch; however, the method blank cannot be use to determine A_R but A_R must be determined using reagent blanks that were analyzed prior to the current preparation batch.

Calculations When the Alpha-Particle Peaks of Po-209 and 210 Overlap.

When the Po-209 and Po-210 peaks overlap, three regions of interest are defined (ROI_1, ROI_2 and ROI_3) as described in Appendix A. In calculating the total efficiency the total number of counts in ROI_2, i.e., $N_{2,S}$, must be corrected for background counts, as in the previous section, and for the counts due to Po-210. This is achieved using the following equation:

$$q_O = \frac{N_{2,C} - \left(\frac{N_{1,C}}{a}\right)}{A_{209} T_S},$$

where the parameter a, derived in Appendix A, is given by

$$a = \frac{N_{2,C} + \sqrt{N_{2,C}^2 - 4N_{1,C}N_{3,C}}}{2N_{3,C}},$$

and

$$N_{i,C} = N_{i,S} - N_{i,B}\,\frac{T_S}{T_B} \quad (i = 1, 2).$$

The calculations for the tracer recovery, $?_T$, and the Po-210 activity, A_{210}, are the same as in the previous section.

11.0 Quality Control.

(incomplete)

11.1 Background.

Every day a 60 minute background spectrum must be collected for each detector. Once a month (incomplete).

11.2 Contamination, Precision, and Accuracy.

Before any samples can be collected, prepared, and analyzed, quality control data must be collected. This quality control data falls within three general classes: data pertaining to the possible contamination of equipment or the reagents, data characterizing the precision of the method, and data characterizing the accuracy of the method. These data are used to characterize the quality of the analytical data of all of the samples in a preparation batch.

11.2.1 **Contamination Criteria.** Various reagents are used to prepare a sample for analysis, and, as a consequence, it is clear that, in general, the reagents will contribute to the Po-210 activity of the prepared sample. Thus, it is necessary to determine the level of Po-210 activity in the reagents both to correct for the Po-210 activity contribution of the reagents to the prepared sample and to compare the compare the Po-210 activity of a method blank with the expected Po-210 reagent activity to determine whether contamination has occurred. In order to do this, a series a reagent blanks must be analyzed to determine the contribution of the reagents to the Po-210 activity of the prepared sample. In the method described in this work a reagent blank and a method blank are prepared in exactly the same way, the only difference being that reagent blanks are prepared prior to the preparation and analysis of any samples and one method blank is included in every preparation batch and is analyzed in the same way as the other samples of the preparation batch. A reagent blank or method blank is prepared using 1 liter of polished water (instead of a sample of groundwater) that is acidified with that amount of nitric acid that is used to pre-acidify a sample of groundwater. (In this method 1 mL of conc. nitric acid is used to pre-acidify each liter of groundwater). Ten reagent blanks were analyzed for Po-210 activity, and the results are given in Table 1 along with the mean and standard deviation of the data.

When a method blank is analyzed, the Po-210 activity due to the reagents is subtracted from the measured Po-210 activity of the method blank. Thus, the Po-210 activity of the analyzed method blank should be close to zero. However, because of statistical error, the method blank will usually deviate, either positively or negatively, from zero. It is clear that the standard deviation of the method blank Po-210 activity is exactly the same as the reagent blank Po-210 standard deviation. The Po-210 activity of the method blank is considered to be within control limits if it is within 2 standard deviations of zero. The Po-210 activity is considered to be within the warning control limits when it deviates by more than 2 standard deviations from zero but is within 3 standard deviations of zero. The Po-210 activity is considered to be in the error when it deviates by more 3 standard deviations from zero. The warning and error limits are given in Table 1.

An error level in a method blank may indicate that detector contamination has occurred, that the reagents have been contaminated with Po-210 due to some

laboratory error, that the Po-210 activity of a new lot of reagents is different from the previous lot, having either increased or decreased, or that some combination of these three sources of error have occurred. Normally, detector contamination can be identified with the daily background check, and will not be considered further as a source of error in the method blank. A method blank with a Po-210 activity that is too high (more than 3s above zero) may indicate that one or more of the reagents has been contaminated with Po-210 or that a new lot of reagents contains more Po-210 activity than a previous lot. An analysis of the various reagents may be necessary to distinguish between these possibilities. A method blank with a Po-210 activity that is too low (less than 3s below zero) may indicate that a new lot of reagents contains less Po-210 activity than a previous lot. If it is suspected that the activity of Po-210 in the reagents has significantly changed, a new series of reagent blanks must be analyzed in order to determine the Po-210 activity which must be subtracted from the prepared samples in order to get the Po-210 activities of the original samples.

Table 1. Po-210 Activity of Reagents (data is incomplete).

Sample	File	Date	% tracer recovery	Reagent activity (mBq)
1	Alph0494.spc	7/14/00	43.75	2.831
2	Alph0495.spc	7/14/00	45.27	2.998
3	Alph0496.spc	7/14/00	43.81	2.871
4				
5				
6				
7				
8				
9				
10				
Mean.				
Standard deviation, s.				
Method blank warning limits, ±2s.				
Method blank error limits, ±3s.				

11.2.2 **Precision Criteria.** In order to characterize the precision of the method, a series of replicates must be analyzed, and the mean and standard deviation of the differences in Po-210 activity between pairs of replicates must be calculated. The Po-210 activities of ten pairs of replicates and their differences and the corresponding mean and standard deviation are given in Table 2. When the Shewart method is used to characterize the precision of the method, a pair of replicates is included in every preparation batch. When the replicates are analyzed, the difference between the Po-210 activities of the replicates is calculated. The difference is considered to be within control limits if it is within 2.51 standard deviations of the mean. The difference is considered to be within the warning control limits when it deviates by more than 2.51 standard deviations from the mean but is within 3.57 standard deviations of the mean. The difference is considered to be in the error when it deviates by more 3.57 standard deviations from the mean. The warning and error limits are given in Table 2.

Table 2. Replicate Analyses of Po-210 solutions (data is incomplete).

Sample	File	Date	% tracer recovery	Po-210 activity (mBq/L)	Activity Difference (mBq/L)
1a	Alph0494.spc	7/14/00		43.75	2.8309597
1b	Alph0495.spc	7/14/00		45.27	
2a	Alph0496.spc	7/14/00		43.81	2.871
2b					
3a					
3b					
4a					
4b					
5a					
5b					
6a					
6b					
7a					
7b					
Mean.					
Standard deviation.					
Replicate warning limits, ±2.51s.					
Replicate error limits, ±3.27s					

11.2.3 **Accuracy Criteria.** In order to characterize the accuracy of the method, a series of laboratory control samples must be analyzed. The results for ten laboratory control samples are given in Table 3. This table includes the actual Po-210 activity added to the sample, the Po-210 activity as determined by this method, the percent error for each laboratory control sample and the mean and standard deviation of percent errors for the ten samples. Ideally, the mean should be zero.

The percent error is considered to be within control limits if it is within 2 standard deviations of the mean. The percent error is considered to be within the warning control limits when it deviates by more than 2 standard deviations from the mean but is within 3 standard deviations of the mean. The percent error is considered to be in the error when it deviates by more 3 standard deviations from the mean. The warning and error limits are given in Table 3.

11.3 **Action To Be Taken When a Warning or Error Limit Has Been Exceeded.**

(Incomplete)

12.0 Appendix A.

At times the peaks due to Po-209 and Po-210 overlap slightly in the alpha spectrum—the low energy tail of the Po-210 peak overlaps the high-energy part of the Po-209 peak. Since the chemistry of Po-209 and 210 is nearly identical, the two isotopes should deposit on the Ni disc in such a way that the functional forms of the two peaks have the same shape. More specifically, the function for the Po-209 peak, F_{209}, and the function for the Po-210 peak, F_{210}, should be related by

$$F_{209}(E_i - \Delta E), = a\, F_{210}(E_i) \quad \text{(for all } i\text{)}, \tag{A1}$$

where E_i is alpha-particle energy of the ith channel, a is a proportionality constant, and ΔE is the energy difference between corresponding points on the two peaks, i.e., ΔE is the energy by which the two peaks are offset from one another. For example, if $E_{peak,209}$ and $E_{peak,210}$ are the energies of the maxima of F_{209} and F_{210}, respectively, then $\Delta E = E_{peak,210} - E_{peak,209}$. Summing both sides of equation (A1) over all channels yields

$$\Sigma_{all\ i}\, F_{209}(E_i) = a \Sigma_{all\ i}\, F_{210}(E_i),$$

or

$$N_{209,C} = aN_{210,C},$$

where $N_{209,C}$ and $N_{210,C}$ are the total counts of Po-209 and Po-210, respectively. The subscript "C" is used hear and below to denote counts that have been corrected for background. It is clear that a is just the ratio of the total amount of Po-209 to the total amount of Po-210 in the sample.

Ordinarily, if the two peaks do not overlap, one can just define two non-overlapping regions of interest (ROI), or energy intervals, each of which encompasses one of the two peaks, and integrate the counts due to Po-209 and Po-210 over their respective ROIs to get the relative amounts of Po-209 and Po-210 in the sample. However, if the peaks overlap, as in Figure 4, such a procedure will not yield accurate results. As seen in Figure 5 above the maximum energy for Po-209, $E_{209,max}$, all of the counts are due to Po-210. Thus, it is useful to define an ROI, named ROI_3, which ranges from a value slightly greater than $E_{209,max}$, call it $E_{209,max} + d$, to a value slightly greater than $E_{210,max}$, call it $E_{210,max} + d$, where d is the same in both cases.; thus, ROI_3 is given by

$$(E_{209,max} + d, E_{210,max} + d).$$

Notice that the length of this interval is just ΔE, the offset energy between the two peaks. The number of counts in this interval, denoted $N_{3,C}$, is just

$$N_{3,C} = \Sigma_{ROI_3} F_{210}(E_i) = N_{3,210} \tag{A2}$$

where Σ_{ROI_3} represents a summation over all of the channels in interval ROI_3, and since all of the counts are due to Po-210, $N_{3,210}$ is just the number of Po-210 counts in interval ROI_3.

It is convenient to define second interval, interval ROI_2, which is given by

$$(E_{209,max} + d - \Delta E, E_{210,max} + d - \Delta E).$$

Intervals ROI_2 and ROI_3 are adjacent to one another, and it is clear from equation (A1) that ROI_2 has the same relationship to F_{209} that ROI_3 has to F_{210}. Thus, it is clear that

$$\Sigma_{ROI_2} F_{209}(E_i) = a \Sigma_{ROI_3} F_{210}(E_i),$$

which simplifies to

$$N_{2,209} = aN_{3,210}, \tag{A3}$$

where $N_{2,209}$ is the number of Po-209 counts in interval ROI_2. Likewise, $N_{1,209}$, the number of Po-209 counts in the interval ROI_1, defined as

$$(E_{209,max} + d - 2?E, E_{210,max} + d - 2?E),$$

is proportional, $N_{2,210}$, to the number of Po-210 counts in interval ROI_2

$$N_{1,209} = aN_{2,210} \quad \text{(A4)}$$

The total number of counts in interval ROI_2, $N_{2,C}$, is given by

$$N_{T,2} = N_{209,2} + N_{210,2}. \quad (5)$$

Likewise, the total number of counts in interval ROI_3 , is given

$$N_{1,C} = N_{1,209} + N_{1,210},$$

where $N_{1,210}$ is the number of Po-210 counts in interval ROI_3. Often it is the case that $N_{2,210} = 0$, i.e., for all practical purposes, there are no counts due to Po-210 in interval ROI_1, so that the above equation becomes

$$N_{1,C} = N_{1,209}. \quad \text{(A6)}$$

Combining equations (A2), (A3), (A4), (A5), and (A6) yields

$$N_{3,C}a^2 - N_{2,C}a + N_{1,C} = 0.$$

Solving this equation for a gives

$$a = \frac{N_{2,C} \pm \sqrt{N_{2,C}^2 - 4N_{1,C}N_{3,C}}}{2N3_{3,C}}.$$

It is clear that the "+" sign must used since if $N_{1,C} = 0$, $a = N_{2,C}/N_{3,C}$, as would be expected. Thus, a can be determined from the total number of counts in each of the intervals ROI_1, ROI_2, and ROI_3, and since $N_{1,209}$ is just $N_{1,C}$, equation (A4) allows for the calculation of $N_{2,210}$, which by equation (A5) is the number of counts that must be subtracted from $N_{2,C}$ to give $N_{2,209}$.

13.0 References.

13.1 Procedure Po-02-RC, Polonium in water, vegetation, soil, and air filters, HASL-200, 28th Edition, Environmental Measurements Laboratory, United States Department of Energy.

13.2 Specification 7.16, *ibid*.

13.3 Fainberg, A. A. and Haring M. M., *Record Chem. Progr.* **14**, 157-74 (1953).

13.4 Govet, G. J. S., *Anal. Chim. Acta* **25**, 69-80 (1961).

13.5 Ha?ssinsky, M., *J. Chim. Phys.* **34**, 94-95 (1937).

13.6 Ha?ssinsky, M., *J. Chim. Phys.* **30**, 27-46 (1933).

13.7 Langmyhr, F. J. and Graff, P. R., Studies in the Spectrophotometric Determination of Silicon in Materials Decomposed by Hydrofluoric Acid I. Loss of Silicon by Decomposition with Hydrofluoric acid, *Anal. Chim. Acta* **21**, 334-339 (1959).

13.8 Langmyhr, F. J. and Sveen, S., Decomposability in Hydrofluoric Acid of the Main and Some Minor and Trace Minerals of Silicate Rocks, *Anal. Chim. Acta* **32**, 1-7 (1965).

13.9 Langmyhr, F. J. and Paus, P. E., The Analysis of Inorganic Siliceous Materials by Atomic Absorption Spectrophotometry and the Hydrofluoric Acid Decomposition Technique, *Anal. Chim. Acta* **43**, 397-408 (1968).

13.10 Sill, C. W. and Olsen, D. G., Sources and Prevention of Recoil Contamination of Solid-State Detectors, *Anal. Chem.* **42**, 1596-1607 (1970).

13.11 Tarutani, T, Polymerization of Silicic Acid: A Review, *Analytical Sciences* 5, 245-252 (1989)

13.12 Weast, R. C., *CRC Handbook of Chemistry and Physics*, 57th Edition, CRC Press, Boca Raton, Florida (1976).

13.13 Buschbeck, E. C., *Gmelin Handbook of Inorganic and Organometallic Chemistry*, Polonium Supplement Volume 1, 8th Edition, Springer-Verlag, Berlin (1990).

14.0 Figures.

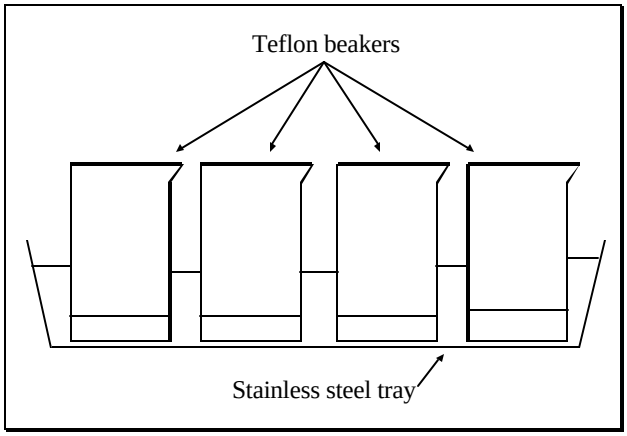

Figure 1. Hot-Water bath for Teflon Beakers.

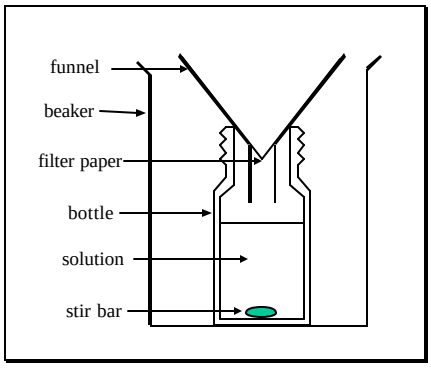

Figure 2. Filter Setup.

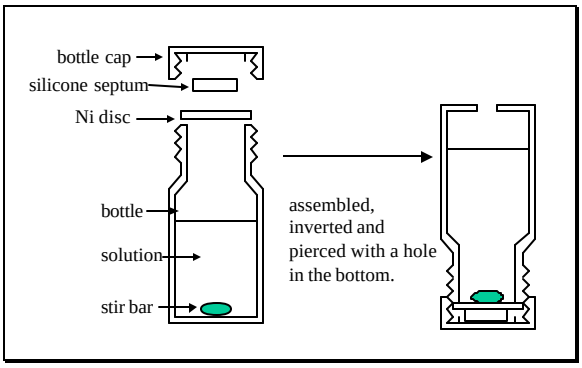

Figure 3. Deposition Cell.

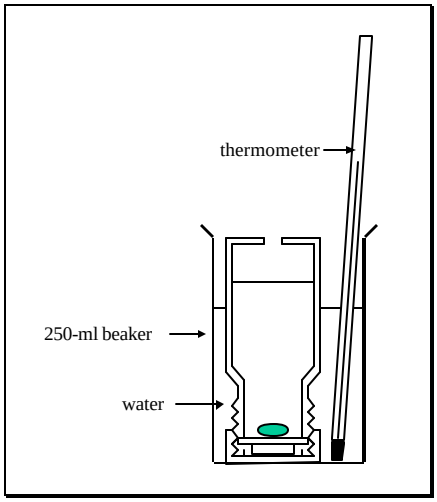

Figure 4. Hot-Water Bath for Deposition Cell.

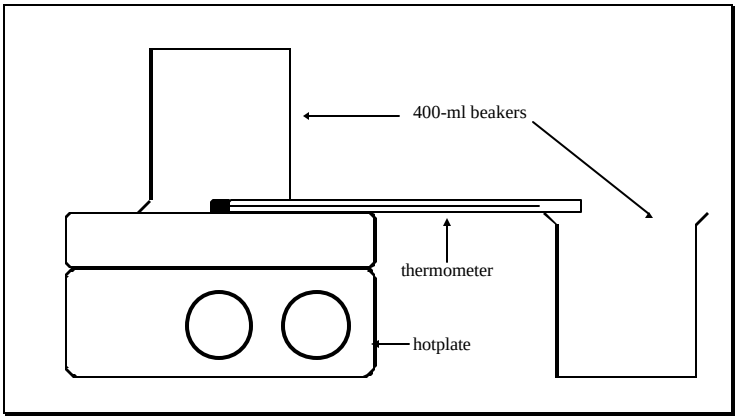

Figure 5. Apparatus for Oxidizing Polonium on Ni disc.

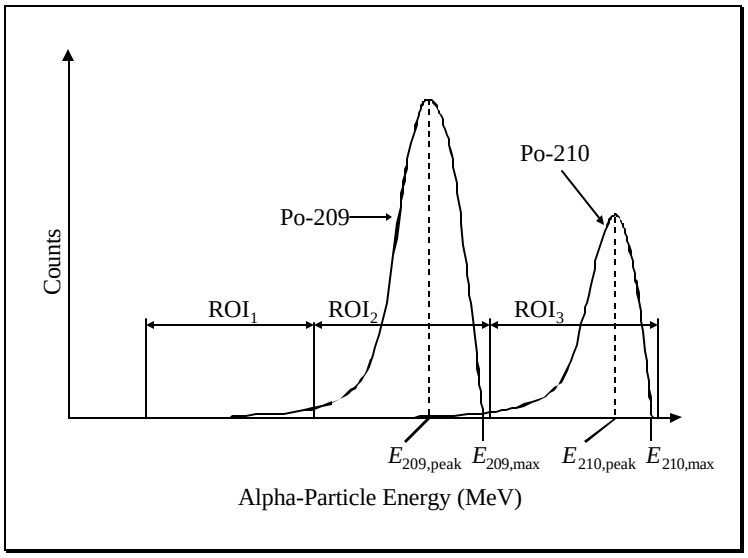

Figure 6. Polonium Alpha Spectrum.

Written by: _____ Date: _____

Title: _____

Unit: _____

Reviewed by: _____ Date: _____

Title: _____

Unit: _____

Approved by: _____ Date: _____

Title: _____

Unit: _____

Appendix B

Radiochemical Data.

Table B1. Gross alpha, gross beta, and Rn-222 activities of ground water samples.

Samp. no.*	location	PWSID no.†	Gross alpha (pCi/L)	Gross Beta (pCi/L)	Rn-222 (pCi/L)
78109	Lake Mills Well #6	12801085	11 ± 2	6.2 ± 1.4	180 ±20
78110	Johnson Creek Well #2	12801074	13 ± 2	6.0 ± 1.3	450 ± 30
78111	Johnson Creek Well #3	12801074	22 ± 3	12 ± 2	380 ± 30
78112	Lake Mills Well #5	12801085	14 ±2	8.3 ± 1.6	340 ± 30
78113	Lake Mills Well #4	12801085	13 ± 2	5.9 ± 1.5	570 ± 40
78147	Hustiford Waterworks Well #2	11401489	19 ± 3	21 ± 2	214 ± 16
78148	Hustiford Waterworks Well #3	11401489	40 ± 4	20 ± 2	183 ± 15
78149	Reeseville Waterworks Well #1	11401533	5 ± 2	4.4 ± 1.3	750 ± 30
78150	Reeseville Waterworks Well #2	11401533	22 ± 3	9.4 ± 1.6	600 ± 20
78173	Pell Lake Sanitary District #1	26514697	64 ± 4	29 ± 2	270 ± 20
78174	Country Estates Comm. Assoc. Well #4	26501277	15 ± 2	9.9 ± 1.1	165 ± 15
78175	Union Grove Waterworks Well #4	25202001	30 ± 3	15 ± 1	140 ± 10
78176	Union Grove Waterworks Well #5	25202001	23 ± 3	14 ± 1	160 ± 20
78177	Southern Wisconsin Center Well #3	25201990	29 ± 3	15 ± 1	130 ± 10
78178	Waterford Waterworks Well #3	25202023	34 ± 3	19.0 ± 1.4	250 ±20
78254	Winneconne Waterworks Well #1	47103540	48 ± 3	16 ± 1	400 ± 20
78255	Winneconne Waterworks Well #2	47103540	30 ± 3	12 ± 1	530 ± 20
78256	Berlin Waterworks Well #4	42402162	24 ± 2	12 ±1	430 ± 20
78257	Berlin Waterworks Well #5	42402162	20 ± 2	9.6 ± 1.0	160 ± 10
78258	Berlin Waterworks Well #6	42402162	18 ± 2	6.9 ± 0.9	1360 ± 40
78259	Princeton Waterworks Well #1	42402195	33 ± 2	12 ± 1	300 ± 20
78260	Princeton Waterworks Well #2	42402195	28 ± 2	14 ± 1	330 ± 20
78319	Bellevue Well #1	40504596	39 ± 4	25.0 ± 1.4	310 ± 20
78320	Bellevue Well #2	40504596	36 ± 3	20.6 ± 1.4	540 ±20
78321	Bellevue Well #3	40504596	66 ± 4	29.5 ± 1.4	1010 ± 30
78322	Bellevue Well #3	40504596	68 ± 5	32.3 ± 1.5	330 ± 20
78323	Allouez Well #1	40504552	21 ± 3	16 ±1	620 ± 30
78324	Allouez Well #2	40504552	18 ± 3	13 ± 1	460 ± 20
78325	Allouez Well #5	40504552	13 ± 2	12 ± 1	280 ± 20
78326	Allouez Well #6	40504552	44 ± 5	22.1 ± 1.4	510 ± 20
78327	Allouez Well #7	40504552	51 ± 4	20.5 ± 1.3	680 ± 30

*Indicates the number assigned to the sample by the Radiochemistry Unit of the Wisconsin State Laboratory of Hygiene.

†Indicates the public water system identification number assigned to the utility by the Wisconsin Department of Natural Resources.

Table B2. U-234, U-235, and U-238 activities of ground water samples.

Samp. no.*	location	PWSID no.†	U-234 (pCi/L)	U-235 (pCi/L)	U-238 (pCi/L)
78109	Lake Mills Well #6	12801085	1.69 ± 0.05	0.02 ± 0.01	0.31 ± 0.02
78110	Johnson Creek Well #2	12801074	1.37 ± 0.05	0.02 ± .01	0.20 ± 0.02
78111	Johnson Creek Well #3	12801074	0.29 ± 0.02	0.01 ± 01	0.04 ± 0.01
78112	Lake Mills Well #5	12801085	2.29 ± 0.06	0.01 ± 0.01	0.21 ± 0.02
78113	Lake Mills Well #4	12801085	2.44 ± 0.06	0.02 ± 0.01	0.32 ± 0.02
78147	Hustiford Waterworks Well #2	11401489	0.82 ± 0.03	0.01 ± 0.01	0.09 ± 0.01
78148	Hustiford Waterworks Well #3	11401489	1.26 ± 0.04	0.01 ± 0.01	0.30 ± 0.02
78149	Reeseville Waterworks Well #1	11401533	1.63 ± 0.05	0.01 ± 0.01	0.21 ± 0.02
78150	Reeseville Waterworks Well #2	11401533	3.08 ± 0.07	0.02 ± 0.01	0.46 ± 0.02
78173	Pell Lake Sanitary District #1	26514697	0.09 ± 0.01	0.00 ± 0.01	0.01 ± 0.01
78174	Country Estates Comm. Assoc. Well #4	26501277	0.04 ± 0.01	0.00 ±0.01	0.01 ± 0.01
78175	Union Grove Waterworks Well #4	25202001	2.47 ± 0.07	0.02 ± 0.01	0.17 ± 0.02
78176	Union Grove Waterworks Well #5	25202001	2.40 ± 0.06	0.01 ± 0.01	0.18 ± 0.02
78177	Southern Wisconsin Center Well #3	25201990	2.05 ± 0.12	0.01 ± 0.01	0.16 ± 0.03
78178	Waterford Waterworks Well #3	25202023	2.50 ± 0.06	0.01 ± 0.01	0.22 ± 0.02
78254	Winneconne Waterworks Well #1	47103540	15.70 ± 0.23	0.09 ± 0.01	1.83 ± 0.05
78255	Winneconne Waterworks Well #2	47103540	10.30 ± 0.17	0.07 ± 0.01	1.24 ± 0.04
78256	Berlin Waterworks Well #4	42402162	2.05 ± 0.06	0.02 ± 0.01	0.32 ± 0.02
78257	Berlin Waterworks Well #5	42402162	1.61 ± 0.05	0.02 ± 0.01	0.23 ± 0.02
78258	Berlin Waterworks Well #6	42402162	4.62 ± 0.09	0.04 ± 0.01	0.69 ± 0.03
78259	Princeton Waterworks Well #1	42402195	1.62 ± 0.05	0.01 ± 0.01	0.23 ± 0.02
78260	Princeton Waterworks Well #2	42402195	1.92 ± 0.05	0.02 ± 0.01	0.31 ± 0.0.
78319	Bellevue Well #1	40504596	4.86 ± 0.21	0.02 ± 0.01	0.32 ± 0.04
78320	Bellevue Well #2	40504596	4.47 ± 0.18	0.02 ± 0.01	0.28 ± 0.04
78321	Bellevue Well #3	40504596	6.34 ± 0.06	0.03 ± 0.01	0.33 ± 0.01
78322	Bellevue Well #3	40504596	5.21 ± 0.05	0.03 ± 0.01	0.43 ± 0.02
78323	Allouez Well #1	40504552	3.64 ± 0.16	0.01 ± 0.01	0.21 ± 0.03
78324	Allouez Well #2	40504552	2.18 ± 0.12	0.02 ± 0.01	0.12 ± 0.02
78325	Allouez Well #5	40504552	0.11 ± 0.02	0.01 ± 0.01	2.28 ± 0.12
78326	Allouez Well #6	40504552	0.19 ± 0.03	0.01 ± 0.01	3.64 ± 0.16
78327	Allouez Well #7	40504552	0.23 ± 0.03	0.02 ± 0.01	4.53 ± 0.19

*Indicates the number assigned to the sample by the Radiochemistry Unit of the Wisconsin State Laboratory of Hygiene.

†Indicates the public water system identification number assigned to the utility by the Wisconsin Department of Natural Resources.

Table B3. Th-228, Th-230, and Th-232 activities of ground water samples.

Samp. No.	location	PWSID no.†	Th-228‡ (pCi/L)	Th-230 (pCi/L)	Th-232 (pCi/L)
78109	Lake Mills Well #6	12801085	0.069 ± 0.008	0.014 ± 0.005	0.002 ± 0.002
78110	Johnson Creek Well #2	12801074	0.010 ± 0.013	0.014 ± 0.005	0.002 ± 0.002
78111	Johnson Creek Well #3	12801074	0.004 ± 0.014	0.023 ± 0.008	0.002 ± 0.005
78112	Lake Mills Well #5	12801085	0.27 ± 0.07	0.017 ± 0.003	0.003 ± 0.002
78113	Lake Mills Well #4	12801085	0.098 ± 0.052	0.019 ± 0.004	0.001 ± 0.002
78147	Hustiford Waterworks Well #2	11401489	0.029 ± 0.004	0.020 ± 0.003	0.003 ± 0.002
78148	Hustiford Waterworks Well #3	11401489	0.022 ± 0.005	0.019 ± 0.003	0.002 ± 0.001
78149	Reeseville Waterworks Well #1	11401533	0.030 ± 0.003	0.009 ± 0.002	0 ± 0.001
78150	Reeseville Waterworks Well #2	11401533	-0.01 ± 0.01	0.012 ± 0.003	0.002 ± 0.001
78173	Pell Lake Sanitary District #1	26514697	-0.02 ± 0.01	0.016 ± 0.003	0.001 ± 0.001
78174	Country Estates Comm. Assoc. Well #4	26501277	0.013 ± 0.003	0.014 ±0.003	-0.022 ± 0.001
78175	Union Grove Waterworks Well #4	25202001	0.005 ± 0.008	0.025 ± 0.005	0.004 ± 0.002
78176	Union Grove Waterworks Well #5	25202001	0.030 ± 0.008	0.010 ± 0.006	0.003 ± 0.003
78177	Southern Wisconsin Center Well #3	25201990	0.062 ± 0.014	0.013 ± 0.003	0.004 ± 0.002
78178	Waterford Waterworks Well #3	25202023	0.008 ± 0.008	0.043 ± 0.007	0.002 ± 0.003
78254	Winneconne Waterworks Well #1	47103540	0.010 ± 0.004	0.016 ± 0.005	-0.002 ± 0.003
78255	Winneconne Waterworks Well #2	47103540	0.001 ± 0.005	0.021 ± 0.006	0.001 ± 0.003
78256	Berlin Waterworks Well #4	42402162	0.27 ± 0.06	0.012 ± 0.003	0.0003± 0.001
78257	Berlin Waterworks Well #5	42402162	0.012 ± 0.004	0.010 ± 0.003	-0.001 ± 0.002
78258	Berlin Waterworks Well #6	42402162	0.013 ± 0.004	0.010 ± 0.004	0.001 ± 0.003
78259	Princeton Waterworks Well #1	42402195	0.28 ± 0.07	0.017 ± 0.004	-0.003 ± 0.002
78260	Princeton Waterworks Well #2	42402195	—	—	—
78319	Bellevue Well #1	40504596	0.57 ± 0.04	0.030 ± 0.003	0.004 ± 0.002
78320	Bellevue Well #2	40504596	0.40 ± 0.03	0.011 ± 0.002	0 ± 0.001
78321	Bellevue Well #3	40504596	0.50 ± 0.05	0.015 ± 0.004	-0.004 ± 0.002
78322	Bellevue Well #3	40504596	0.49 ± 0.05	0.023 ± 0.004	0.001 ± 0.002
78323	Allouez Well #1	40504552	0.41 ± 0.04	0.021 ± 0.006	-0.005 ± 0.004
78324	Allouez Well #2	40504552	0.16 ± 0.02	0.024 ± 0.007	0.012 ± 0.004
78325	Allouez Well #5	40504552	0.23 ± 0.04	0.016 ± 0.004	0 ± 0.002
78326	Allouez Well #6	40504552	0.41 ± 0.04	0.015 ± 0.004	0.002 ± 0.002
78327	Allouez Well #7	40504552	0.22 ± 0.02	0.035 ± 0.004	0.008 ± 0.002

A dash "—" indicates that the sample has not yet been analyzed for that particular nuclide.
*Indicates the number assigned to the sample by the Radiochemistry Unit of the Wisconsin State Laboratory of Hygiene.
†Indicates the public water system identification number assigned to the utility by the Wisconsin Department of Natural Resources.
‡The activity of Th-228 has been corrected for the ingrowth of Th-228 due to Ra-228 and Ac-228.

Table B4. Ra-226, Ra-228, and Po-210 activities of ground water samples.

Samp. No.	location	PWSID no.†	Ra-226 (pCi/L)	Ra-228 (pCi/L)	Po-210 (pCi/L)
78109	Lake Mills Well #6	12801085	1.87 ± 0.15	2.1 ± 0.6	0.0180 ± 0.0006
78110	Johnson Creek Well #2	12801074	2.08 ± 0.15	1.5 ± 0.5	0.0870 ± 0.0011
78111	Johnson Creek Well #3	12801074	4.5 ± 0.2	3.6 ± 0.7	0.0180 ±0.0007
78112	Lake Mills Well #5	12801085	3.0 ± 0.2	1.8 ± 0.6	0.0179 ± 0.0005
78113	Lake Mills Well #4	12801085	1.2 ± 0.1	1.1 ± 0.5	0.0625 ± 0.0006
78147	Hustiford Waterworks Well #2	11401489	3.7 ± 0.2	3.8 ± 0.7	-0.0085 ± 0.0058*
78148	Hustiford Waterworks Well #3	11401489	7.1 ± 0.2	6.7 ± 0.9	—
78149	Reeseville Waterworks Well #1	11401533	0.92 ± 0.10	0.5 ± 0.5	0.0154 ± 0.0058*
78150	Reeseville Waterworks Well #2	11401533	4.4 ± 0.2	2.5 ± 0.7	0.0202 ± 0.0058*
78173	Pell Lake Sanitary District #1	26514697	13.5 ± 0.4	7.7 ± 0.9	0.0059 ± 0.0002
78174	Country Estates Comm. Assoc. Well #4	26501277	3.0 ± 0.2	1.8 ± 0.6	0.0033 ± 0.0002
78175	Union Grove Waterworks Well #4	25202001	5.8 ± 0.2	3.2 ± 0.9	0.0035 ± 0.0002
78176	Union Grove Waterworks Well #5	25202001	3.7 ± 0.2	2.1 ± 0.7	0.0036 ± 0.0002
78177	Southern Wisconsin Center Well #3	25201990	3.9 ± 0.2	3.1 ± 0.8	0.0045 ± 0.0002
78178	Waterford Waterworks Well #3	25202023	7.1 ± 0.2	3.1 ± 0.8	0.0039 ± 0.0003
78254	Winneconne Waterworks Well #1	47103540	5.5 ± 0.2	4.3 ± 0.9	0.0146 ± 0.0003
78255	Winneconne Waterworks Well #2	47103540	2.34 ± 0.15	2.1 ± 0.8	0.0250 ± 0.0003
78256	Berlin Waterworks Well #4	42402162	2.9 ± 0.2	3.1 ± 0.8	0.0786 ± 0.0004
78257	Berlin Waterworks Well #5	42402162	2.29 ± 0.16	2.5 ± 0.8	0.0602 ± 0.0004
78258	Berlin Waterworks Well #6	42402162	2.80 ± 0.16	1.4 ± 0.7	0.0146 ±0.0002
78259	Princeton Waterworks Well #1	42402195	5.1 ± 0.2	4.1 ± 0.9	0.0225 ± 0.0003
78260	Princeton Waterworks Well #2	42402195	5.6 ± 0.2	3.8 ± 0.9	0.0120 ± 0.0002
78319	Bellevue Well #1	40504596	8.6 ± 0.3	6.0 ± 1.0	0.0091 ± 0.0002
78320	Bellevue Well #2	40504596	7.4 ± 0.3	4.9 ± 0.9	—
78321	Bellevue Well #3	40504596	15.2 ± 0.4	5.3 ± 1.1	0.0179 ± 0.0005
78322	Bellevue Well #3	40504596	17.0 ± 0.4	9.0 ± 1.2	0.0054 ± 0.0001
78323	Allouez Well #1	40504552	5.1 ± 0.2	3.4 ± 0.8	—
78324	Allouez Well #2	40504552	3.7 ± 0.2	3.1 ± 0.8	—
78325	Allouez Well #5	40504552	2.3 ± 0.2	2.2 ± 0.9	—
78326	Allouez Well #6	40504552	9.2 ± 0.3	4.6 ± 1.0	—
78327	Allouez Well #7	40504552	9.3 ± 0.3	4.5 ± 1.2	—

A dash "—" indicates that the sample has not yet been analyzed for that particular nuclide.
*Indicates the number assigned to the sample by the Radiochemistry Unit of the Wisconsin State Laboratory of Hygiene.
†Indicates the public water system identification number assigned to the utility by the Wisconsin Department of Natural Resources.

Appendix C

Model for Gross Alpha Measurement.

Model of Gross Alpha Measurement.

Introduction.

Figure 1 shows the idealized geometry of a pancake-style gas proportional detector used for gross alpha measurements. The system consists of a planchet, a solid film containing the nuclides of interest, a layer of air, the window of the detector, and the counting gas within the detector. (The dimensions are not drawn to scale.). The gas within the detector is typically a mixture argon and methane. In a pancake-style detector the gas is the active region of the detector. Electrons produced in the gas by ionization of gas molecules by alpha particles migrate toward the detector anode (the detector window is the cathode). Near the surface of the anode these electrons are accelerated and, as a consequence, gain enough energy to ionize more gas molecules; thus, the signal of a single electron produce by an alpha particle can be multiplied several hundred thousand times. These electrons are collected at the anode, leading to a measurable voltage pulse. In a windowless 2p gas proportional detector, there is no layer of air and there is no detector window (the planchet is the cathode), so that practically every electron that an alpha particle emerging from the solid film produces in the gas is multiplied and collected at the anode.

All of the interfaces between the components of the detector system are assumed to be planar and parallel to one another. The origin of the Cartesian coordinate system is located on interface (β). The *z*-axis is perpendicular to the interfaces and is oriented such that its positive axis goes through the solid film. The orientation of the of the x- and y-axes in interface (β) is arbitrary. The thicknesses of the solid film, the air layer, and the detector window are t_F, t_A, and t_W, respectively.

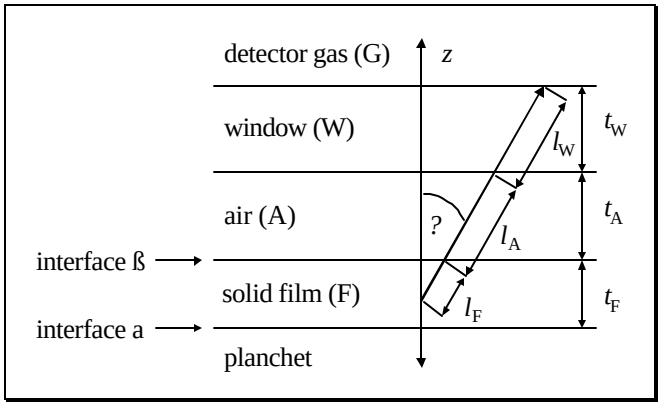

Figure 1. Schematic of Gross Alpha Measurement System.

Condition for Pulse Generation in Gas Proportional Counters.

Alpha particles lose most of their kinetic energy by way of collisions with electrons, collisions between alpha particles and nuclei being relatively rare. Since the mass of an electron is much less than that of an alpha-particle, an alpha particle tends to travel in a relatively straight line through matter. In order to be detected an alpha particle cannot dissipate all of its energy before reaching the detector gas. Experiments

are often performed in which alpha particles are allowed to impinge on a sheet of material of a given film thickness. The thickness of the film determines how many collision the alpha particle will experience on its way through the film—if the film is thick enough, the alpha particle will be stopped within the volume of the film. The number of collisions an alpha particle experiences is related to the total number of electrons per unit area that are presented to the alpha particle. For example, if the material from which the film is constructed has an electronic density of r_F, the total number of electrons per unit area presented to the alpha particle will be equal to the thickness of the material, t_F, multiplied by the electronic density of the material, or $r_F t_F$. The quantity $r_F t_F$ is often given a name such as the "electronic thickness." It is clear that if t_F exceeds some value R, called the range of the alpha particle, then some of the alpha particles will be stopped within the volume of the film. The electronic density of the film is readily calculated using the equation

$$r_F = \sum_{i=1}^{n_F} N_{F,i} Z_{F,i},$$

where $N_{F,i}$,is the number of atoms of the ith type per unit volume in the solid film, $Z_{F,i}$, is the charge on the ith atom, and n_F, is the number of distinct types of atoms in the solid film. The electronic densities of the other components of the detector are calculated in a similar way.

Let the range of an alpha particle of the ith nuclide in the solid film be denoted by $R_{F,i}$. That is, an alpha particle of the ith nuclide can travel a distance $R_{F,i}$ in the solid film before all of its energy is dissipated and it comes to rest. Over the course of such a path the alpha particle experiences an electronic thickness of $r_F R_{F,i}$. When the alpha particle originates within the solid film and reaches and is stopped within the detector gas, the total electronic thickness experienced by the alpha particle is given by

$$r_F l_F + r_A l_A + r_W l_W + r_G l_G,$$

where l_F, l_A, l_W, and l_G are the distances traveled by the alpha particle of the ith nuclide in the solid film, the air layer, the detector window, and the counting gas respectively; and r_F, r_A, r_W, and r_G are the electronic densities of the solid film, the air layer, the detector window, and the counting gas, respectively.

In this model it is assumed that the distance that an alpha particle of a given energy travels is completely characterized by the electronic thickness that is experiences. For example, when an alpha particle of the ith nuclide originates and is stopped within the solid film, the electronic thickness the alpha particle experiences is just $r_F R_{F,i}$ as noted above. Thus, given the assumptions made above, when an alpha particle of the ith nuclide originates within the solid film and is stopped within the counting gas, it is clear that

$$r_F l_F + r_A l_A + r_W l_W + ?_G l_G = r_F R_{F,i}.$$

The alpha particle must travel a certain minimum distance in the detector gas before it can ionize enough of the molecules of the detector gas to cause a detectable pulse. Let this distance be $l_{G,min}$. Consequently, an alpha particle of the ith nuclide generates a pulse whenever

$$r_F l_F + r_A l_A + r_W l_W + r_G l_{G,min} \le r_F R_{F,i}. \quad (1)$$

Since the windowless gas proportional counter does not have a window or an intervening layer of air, the condition for pulse generation in windowless 2π gas proportional detector is obtained by setting l_A and l_W equal to zero in Equation (1).

It is clear that the maximum value with which the alpha particle can deviate from the direction perpendicular to the interface and still be detected will depend on the energy of the alpha particle and, therefore, on the nuclide from which it originates. The maximum angle for an alpha particle of the ith nuclide will be denoted by $q_{max,i}(z)$, and the corresponding solid angle defined by the cone $q = q_{max,i}$ will be

denoted by $\Omega_i(z)$. From Equation (1) it is clear that the condition which determines the maximum angle at which an alpha particle can be emitted and still generate a pulse in the counting gas is given by

$$r_F l_{F,max,i} + r_A l_{A,max,i} + r_W l_{W,max,i} + r_G l_{G,min,i} = r_F R_{F,i}$$

where the subscript "max" is used to denote the maximum possible length that an alpha particle of the *i*th nuclide can attain in the corresponding medium. From Figure 1 it is clear that

$$\cos\theta_{max,i} = \frac{z}{l_{F,max,i}} = \frac{t_A}{l_{A,max,i}} = \frac{t_W}{l_{W,max,i}}.$$

Using the two previous equations, it is readily shown that

$$\cos\theta_{max,i} = \frac{r_F z + r_A t_A + r_W t_W}{r_F R_{F,i} - r_G l_{G,min}}. \quad (2)$$

For solid films exceeding a certain thickness it is apparent that there is a depth in the film, call it $z_{max,i}$, such that alpha particles originating below this depth will dissipate too much of their energy to cause a pulse in the detector. This occurs when $\theta_{max,i}$ goes to zero, or when $\cos\theta_{max,i}$ equals unity. Setting $\cos\theta_{max,i}$ equal to unity gives

$$z_{max,i} = R_{F,i} - \frac{r_A t_A + r_W t_W + r_G l_{G,min}}{r_F}. \quad (3)$$

In this section the solid angle Ω_i in which particle may be emitted from the solid film and still generate a pulse in the detector will be assumed to be a function of *z* only. For a windowless 2π detector such a procedure will lead to accurate results. However, for a pancake style detector for a given value of *z* the solid angle diminishes as the outer edge of the planchet is approached because some of the alpha particles emitted from this region collide with the edge of the planchet and do not reach the detector. The correction due to these "edge effects" will be considered in another section.

Ignoring edge effects, the solid angle in which particles may be emitted and still generate a pulse in the detecor is related to $\cos\theta_{max,i}$ by the following well-known result from solid geometry:

$$\Omega_i(z) = 2\pi(1 - \cos\theta_{max,i}).$$

Substituting Equation (2) into this equation yields

$$\Omega_i(z) = 2\pi\left(1 - \frac{r_F z + r_A t_A + r_W t_W}{r_F R_{F,i} - r_G l_{G,min}}\right) \quad (4)$$

Expressions for $z_{max,i}$ and $W_i(z)$ for the windowless 2p gas proportional detector are obtained by setting t_A and t_W equal to zero in Equations (3) and (4).

Contribution of a Nuclide to the Detector Signal.

In general, the radioactivity in the solid film will not be distributed evenly throughout the volume of the film. Depending upon which nuclides are present and how the film is prepared, the radioactivity may be a function of *z*. In addition, some nuclides may be surface-active, and, as a consequence, tend to migrate to either interface a or interface ß or both. However, for the sake of simplicity, it will be assumed that for a given nuclide and film thickness, t_F, the distribution of the radioactivity can be described by three constants: an activity density at interface a, $s_i^{(a)}$, an activity density at interface ß, $s_i^{(ß)}$, and an activity density in the volume of the film, $s_{S,i}$. The two interfacial activity densities have units of decays per unit time per unit area, and the activity density of the film volume has units of decays per unit time per unit volume. Although these densities are assumed to be independent of the coordinates, they will clearly depend upon the film thickness. If A_i is the total activity of the *i*th nuclide in the solid film (not the pulse rate of the detector), then it is clear that

$$A_i = s_i^{(a)} S + s_i^{(ß)} S + s_{F,i} t_F S. \tag{5}$$

Now, if $t_F < z_{max,i}$, then some of the alpha particles emitted from interface a will be able to reach the counting gas and to cause a pulse in the detector. The activity of the *i*th nuclide in area element *dS* is just $s_i^{(a)} dS$. The fraction of particles emitted that are able to cause a pulse in the detector is just the solid angle in which particles must be emitted to reach the detector, $\Omega_i(z = t_F)$, divided by 4p; thus, the differential pulse rate of the detector due to particles emitted from area element *dS* is given by

$$dI_i^{(a)} = \frac{\Omega_i(z = t_F)}{4p} s_i^{(a)} dS.$$

Integrating this equation using Equation (4) to evaluate $\Omega_i(z = t_F)$ yields the total pulse rate from interface α:

$$I_i^{(a)} = \frac{1}{2}\left(1 - \frac{r_F t_F + r_A t_A + r_W t_W}{r_F R_{F,i} - r_G l_{G,min}}\right) s_i^{(a)} S. \tag{6}$$

From Equation (6) it is readily seen that $I_i^{(a)}$ approaches zero as t_F approaches $z_{max,i}$. Similarly, at interface ß the differential pulse rate is given by

$$dI_i^{(a)} = \frac{\Omega_i(z = 0)}{4p} s_i^{(a)} dS,$$

which, using Equation (4) to evaluate $\Omega_i(z = 0)$, may be integrated to yield

$$I_i^{(b)} = \frac{1}{2}\left(1 - \frac{r_A t_A + r_W t_W}{r_F R_{F,i} - r_G l_{G,min}}\right) s_i^{(b)} S. \tag{7}$$

As would be expected, $I_i^{(β)}$ goes to zero as the electronic thickness of the air and window, $r_A l_A + r_W l_W$, approaches $r_F R_{F,i}. - r_G l_{G,min}$.

Finally, in the volume of the film the differential pulse rate of the detector due to emission of alpha particles of the *i*th nuclide from volume element *dV* at a depth *z* in the film is given by

$$dI_{F,i} = \frac{\Omega_i(z)}{4p} s_{F,i} dV.$$

The solid angle within which an alpha particle of a given energy will cause a pulse in the detector has been considered to be constant over an interface; however, it is clear that in the film the solid angle is a function of *z*, with the solid angle decreasing as the film is traversed from interface ß to interface a. In general, for a particular nuclide two cases can be distinguished. In the first case the solid angle is greater than zero throughout the volume of the solid film. In the second case the solid angle diminishes to zero within the film at $z = z_{max,i}$. In the first case, the integration is over the entire volume of the solid film; in the second case, the integration is only over the volume of the solid film that contributes to the alpha-particle flux reaching the detector. Thus, both cases are covered by the following equation:

$$I_{F,i} = \iint_S \left(\int_0^{\min(t_F, z_{max})} \frac{\Omega_i(z)}{4p} s_{F,i} dz \right) dS,$$

where $z_{max,i}$ is given by Equation (3). Integrating this equation, using Equation (4), yields

$$I_{F,i} = \frac{s_{F,i} S}{2} \left[\left(1 - \frac{r_A t_A + r_W t_W}{r_F R_{F,i} - r_G l_{G,min}} \right) z - \frac{r_F}{2(r_F R_{F,i} - r_G l_{G,min})} z^2 \right] \quad [z = \min(t_F, z_{max})], \tag{8}$$

where the results for the windowless 2π detector are obtained by setting l_A and l_W to zero.

Calibration Plot for Windowless 2p Gas Proportional Detector when the Nuclide used for calibration is not Surface-Active.

A detector is usually calibrated using a particular nuclide. A calibration plot for a detector is a graph of the detector efficiency, given by

$$q_i = \frac{I_{F,i}}{A_i},$$

for the windowless 2π detector, versus the mass of the solid film The mass of the solid film, *m*, is given by

$$m = h_F t_F S,$$

where h_F is the density of the solid film. Substituting this into Equation (11) and dividing by A_i yields the detector efficiency when $t_F < z_{max,i}$:

$$q_i = \frac{1}{2} \left(1 - \frac{r_F m}{2 h_F S (r_F R_{F,i} - r_G l_{G,min})} \right) \quad (t_F \le z_{max}).$$

The result for $t_F > z_{max,i}$ is given by

$$q_i = \left(r_F R_{F,i} - r_G l_{G,\min}\right)\frac{h_F S}{4 r_F m} \quad (t_F > z_{\max}).$$

The initial slope of a calibration plot is given by

$$a = -\frac{r_F}{4h_F S(r_F R_{F,i} - r_G l_{G,\min})},$$

and the *y*-intercept is given by

$$b = \frac{1}{2},$$

which is the result to be expected from the 2p counting geometry.

Before such results can be obtained for the pancake-style gas proportional counter, the effect of the planchet wall on the attenuation of the alpha particle signal must be considered.

The Edge Effect for the Pancake-Style Gas Proportional Counter.

In this section the rate at which alpha particles that collide with the vertical wall of the planchet or the wall of some other sample cell with cylindrical geometry will be determined so that the reduction of the alpha-particle signal due to this "edge effect" may be determined. It will be assumed that the film thickness is much less than the height of the planchet wall. Two coordinate systems will be employed for this purpose. The first coordinate system is coincident will the coordinate system used in Figure 1, except that cylindrical polar coordinates will be employed. Thus, a point in space is located by the angle f, which defines the half-plane inclined at an angle f with respect to the half-plane defined by the *z*-axis and the positive *x*-axis, by the distance r from the *z*-axis, and by the distance *z* along the z-axis. If the radius of the planchet is *r* and the height of the planchet wall is *a*, then the minimum distance from the center of the planchet at which alpha particles begin to collide with the planchet wall is given by

$$r_{\min,i} = r - a\tan q_{\max,i} \qquad (\tan q_{\max,i} \le r/a), \tag{9}$$

where $\tan q_{\max,i}$ is obtained from Equation (2). Since $q_{\max,i}$ is a function of *z*, it is clear that $r_{\min,i}$ is also a function of *z*. The alpha particle activity originating from some point *P* at a distance r from the *z*-axis satisfying the condition $r_{\min,i} < r \le r$ (the region between the dashed circle and the outside edge of the planchet in Figure 2) will be partially attenuated by the planchet wall. The amount by which alpha-particle activity originating from point *P* is attenuated is the subject of the next few paragraphs.

To facilitate the calculation of the alpha particle attenuation by the wall, a second coordinate system will be employed with origin at point *P*. As is illustrated in Figures 2 and 3, the *x*-axis of the second coordinate system is parallel to the *x*-axis of the first coordinate system and the *z*-axis of the second coordinate system is parallel to the *z*-axis of the first coordinate system. Moreover, a spherical polar coordinate system will be used to define the trajectory of the alpha particles. The angle q_P is the angle between the trajectory and the *z*-axis and the angle f_P is the angle between the vertical half-plane containing the trajectory and the half-plane defied by the *z*-axis and the positive *x*-axis.

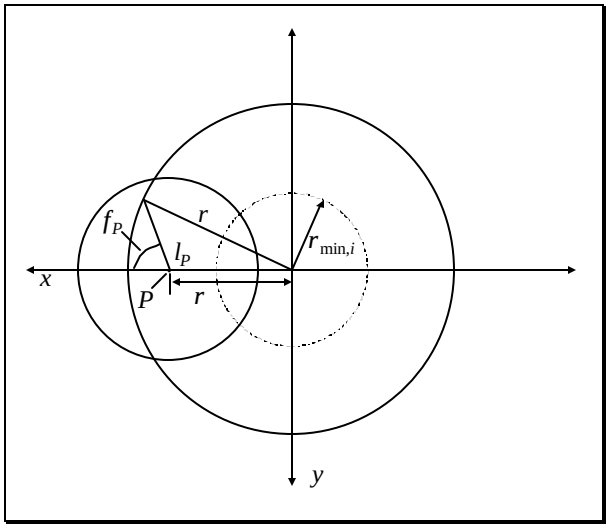

Figure 2. View of planchet from above.

When q_P is very small, the alpha particle will miss the planchet wall. As q is increased, alpha particles which are directed away from the center of the planchet will just begin colliding with the planchet wall when $q_P = q_{P,\min}$, where

$$q_{P,\min} = \tan^{-1}\left(\frac{r - r}{a}\right) \tag{10}$$

To find the number of alpha particles originating from the point P that collide with the planchet wall, one must find the solid angle at point P that is subtended by that portion of the wall that lies between the two cones defined by equations $q_P = q_{P,\min}$ and $q_P = q_{\max,i}$. Let this solid angle be denoted by $\Omega_{P,i}$. In spherical polar coordinates the differential element of a solid angle is given by

$$d\Omega_P = df_P \sin q_P dq_P .$$

Because of symmetry the lower and upper limits of f_P in the integration of the above equation must be equal in magnitude but opposite in sign. Thus, the integration with respect to f_P can be carried out by changing the lower limit to zero and multiplying the result by two. Consequently, if the upper limits of f_P can be expressed as a function q_P, call it $f_{P,\max}$, the above equation is readily integrated to yield

$$\Omega_{P,i} = 2\int_{q_{P,\min}}^{q_{\max,i}} \left(\int_0^{f_{P,\max}} df_P \right) \sin q_P dq_P = 2\int_{q_{P,\min}}^{q_{\max,i}} f_{P,\max} \sin q_P dq_P . \tag{11}$$

The evaluation of $f_{P,\max}$ is the subject of the next paragraph.

Let l_P be the distance from the point P to some point on the planchet wall, as illustrated in Figures 2 and 3. Then, from these figures, it is clear that l_P is related to the angle f_P by

$$(r + l_P \cos f_P)^2 + l_P^2 \sin^2 f_P = r^2 .$$

Solving this equation for $\cos f_P$ yields

$$\cos f_{\mathrm{P}} = \frac{r^2 - r^{\prime 2} - l_{\mathrm{P}}^2}{2 r l_{\mathrm{P}}}. \tag{12}$$

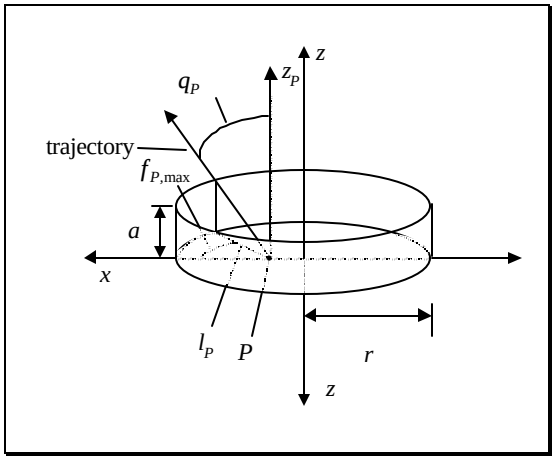

Figure 3.

From Figure 3 it is clear that when $f_{\mathrm{P}} = f_{\mathrm{P,max}}$,

$$\tan q_{\mathrm{P}} = \frac{l_{\mathrm{P}}}{a}.$$

Substituting this result into Equation (12) and solving for $f_{\mathrm{P,max}}$ yields

$$f_{\mathrm{P,max}} = \cos^{-1}\left(\frac{r^2 - r^{\prime 2} - a^2 \tan^2 q_{\mathrm{P}}}{2 r a \tan q_{\mathrm{P}}} \right)$$

the desired result. Further, substituting this result into Equation (11) yields

$$\Omega_{\mathrm{P},i} = 2 \int_{q_{\mathrm{P,min}}}^{q_{\max,\, i}} \cos^{-1}\left(\frac{r^2 - r^{\prime 2} - a^2 \tan^2 q_{\mathrm{P}}}{2 r a \tan q_{\mathrm{P}}} \right) \sin q_{\mathrm{P}}\, dq_{\mathrm{P}}. \tag{13}$$

Since $q_{\mathrm{P,min}}$ is a function of r [Equation (10)] and $q_{\max,i}$ is a function of z [Equation (2)], it is seen that $\Omega_{\mathrm{P},i}$ is independent of the variable f; i.e., $\Omega_{\mathrm{P},i} = \Omega_{\mathrm{P},i}(r, z)$.

The total rate at which alpha particles of the ith nuclide at interface α collide with the planchet wall is given by

$$J_i^{(\mathrm{a})} = s_i^{(\mathrm{a})} \int_{r_{\min,i}}^{r} \left(\int_0^{2p} \left(\frac{1}{4p} \Omega_{\mathrm{P}}(r, z = t_{\mathrm{F}}) \right) df \right) r\, dr.$$

Substituting Equations (9) and (13) into this equation and carrying out the integration with respect to f yields

$$J_i^{(a)} = s_i^{(a)} \int_{r-a\tan q_{\max,i}\big|_{z=t_F}}^{r} \left(\int_{q_{P,\min}}^{q_{\max,i}\big|_{z=t_F}} \cos^{-1}\left(\frac{r^2 - r'^2 - a^2\tan^2 q}{2ar'\tan q} \right) \sin q\, dq \right) r'\, dr',$$

where the subscript "P" has been dropped form q_P in the integrand since no confusion will arise. A similar expression holding for alpha particles emitted from interface (β), the only difference being that $q_{\max,i}$ is evaluated at $z = 0$ instead of $z = t_F$.

In a similar manner the rate at which alpha particles of the ith nuclide in the volume of the solid film collide with the planchet wall is given by

$$J_{F,i} = s_{F,i} \int_0^{\min(t_F, z_{\max})} \left(\int_{r-a\tan q_{\max,i}}^{r} \left(\int_{q_{P,\min}}^{q_{\max,i}} \cos^{-1}\left(\frac{r^2 - r'^2 - a^2\tan^2 q}{2ar'\tan q} \right) \sin q\, dq \right) r'\, dr' \right) dz. \qquad (14)$$

The total detector pulse rate due to the ith nuclide corrected for edge effects, T_i, is just the sum of the contributions of the two interfaces and the solid film minus the corresponding corrections for edge effects; i.e.,

$$T_i = I_i^{(a)} - J_i^{(a)} + I_i^{(ß)} - J_i^{(ß)} + I_{F\,i} - J_{F\,i}.$$

When more than are n nuclides contributing to the detector pulse rate, then the previous equation is summed over all the nuclides to get the total corrected pulse rate:

$$T = \sum_{i=1}^{n} \left(I_i^{(a)} - J_i^{(a)} + I_i^{(ß)} - J_i^{(ß)} + I_{F,i} - J_{F,i} \right).$$

Efficiency of the Pancake-Style Gas Proportional Detector when the Nuclide is not Surface-Active.

As noted above, $s_i^{(a)}$, $s_i^{(ß)}$, and $s_{F,i}$ are functions of the film thickness, t_F. In the special case in which the nuclide is not surface-active, all of the activity of the nuclide is contained within the volume of the film, and both $s^{(a)}$ and $s^{(ß)}$ are zero. Consequently,

$$s_{F,i} = \frac{A_i}{St_F}.$$

Substituting this result into Equations (8) and (14) for the case when $t_{F,i} < z_{\max,i}$ and taking the difference of the two results yields the total activity due to the ith nuclide:

$$T_{F,i} = \frac{A_i}{2}\left\{ \left[\left(1 - \frac{r_A t_A + r_W t_W}{r_F R_{F,i} - r_G l_{G,\min}} \right) - \frac{r_F}{2(r_F R_{F,i} - r_G l_{G,\min})} t_F \right] \right. \qquad (15)$$
$$\left. - \frac{2}{St_F} \int_0^{t_F} \left(\int_{r-a\tan q_{\max,i}}^{r} \left(\int_{q_{P,\min}}^{q_{\max,i}} \cos^{-1}\left(\frac{r^2 - r'^2 - a^2\tan^2 q}{2ar'\tan q} \right) \sin q\, dq \right) r'\, dr' \right) dz \right\} \quad (t_{F,i} < z_{\max,i}).$$

A detector is usually calibrated using a particular nuclide. A calibration plot for a detector is a graph of the detector efficiency, given by

$$q_i = \frac{T_{\mathrm{F},i}}{A_i},$$

versus the mass of the solid film The mass of the solid film, m, is given by

$$m = h_{\mathrm{F}} t_{\mathrm{F}} S,$$

where h_{F} is the density of the solid film. Substituting this into Equation (15) and dividing by A_i yields the detector efficiency when $t_{\mathrm{F}} < z_{\max,i}$:

$$\begin{aligned} q_i = {} & \frac{1}{2}\left[\left(1 - \frac{r_{\mathrm{A}} t_{\mathrm{A}} + r_{\mathrm{W}} t_{\mathrm{W}}}{r_{\mathrm{F}} R_{\mathrm{F},i} - r_{\mathrm{G}} l_{\mathrm{G,min}}}\right) - \frac{r_{\mathrm{F}} m}{2 h_{\mathrm{F}} S (r_{\mathrm{F}} R_{\mathrm{F},i} - r_{\mathrm{G}} l_{\mathrm{G,min}})}\right] \\ & - \frac{h_{\mathrm{F}}}{2m} \int_0^{\frac{m}{h_{\mathrm{F}} S}} \left(\int_{r - a \tan q_{\max,\,i}}^{r} \left(\int_{q_{\mathrm{P,min}}}^{q_{\max,\,i}} \cos^{-1}\left(\frac{r^2 - r^2 - a^2 \tan^2 q}{2ar \tan q} \right) \sin q \, dq \right) r \, dr \right) dz \quad (t_{\mathrm{F}} < z_{\max,\,i}), \end{aligned} \tag{16}$$

which shows that the detected activity decreases monotonically with m for a non-surface-active nuclide when $t_{\mathrm{F}} < z_{\max,i}$.

The y-intercept of the detector efficiency is given by the limit of q_i as the film mass approaches zero. Thus, setting $m = 0$ in the first term of Equation (16) and using L'Hopital's rule to evaluate the limit of the second term in Equation (16) as m approaches zero yields the following equation for the y-intercept:

$$\begin{aligned} \lim_{m \to 0} q_i = {} & \frac{1}{2}\left(1 - \frac{r_{\mathrm{A}} t_{\mathrm{A}} + r_{\mathrm{W}} t_{\mathrm{W}}}{r_{\mathrm{F}} R_{\mathrm{F},i} - r_{\mathrm{G}} l_{\mathrm{G,min}}}\right) \\ & - \frac{1}{S} \int_{r - a \tan q_{\max,\,i}\big|_{z=0}}^{r} \left(\int_{q_{\mathrm{P,min}}}^{q_{\max,\,i}\big|_{z=0}} \cos^{-1}\left(\frac{r^2 - r^2 - a^2 \tan^2 q}{2ar \tan q} \right) \sin q \, dq \right) r \, dr \quad (t_{\mathrm{F}} < z_{\max,\,i}). \end{aligned}$$

A similar result can be derived for the detector efficiency when $t_{\mathrm{F}} = z_{\max}$. Such a process yields

$$\begin{aligned} q_i = {} & \frac{h_{\mathrm{F}} S}{m} \left\{ \frac{1}{2}\left[\left(1 - \frac{r_{\mathrm{A}} t_{\mathrm{A}} + r_{\mathrm{W}} t_{\mathrm{W}}}{r_{\mathrm{F}} R_{\mathrm{F},i}}\right) z_{\max,\,i} - \frac{r_{\mathrm{G}}}{2(r_{\mathrm{F}} R_{\mathrm{F},i} - r_{\mathrm{G}} l_{\mathrm{G,min}})} z_{\max,\,i}^2 \right] \right. \\ & \left. - \frac{1}{S} \int_0^{z_{\max}} \left(\int_{r - a \tan q_{\max,\,i}}^{r} \left(\int_{q_{\mathrm{P,min}}}^{q_{\max,\,i}} \cos^{-1}\left(\frac{r^2 - r^2 - a^2 \tan^2 q}{2ar \tan q} \right) \sin q \, dq \right) r \, dr \right) dz \right\} \quad (t_{\mathrm{F}} \geq z_{\max,\,i}), \end{aligned} \tag{17}$$

which shows that the detector efficiency decreases hyperbolically toward zero as m is increased.

From Equation (16) the derivative of the detector efficiency, q_i, with respect to mass, m, when $t_{\mathrm{F}} > z_{\max}$ is given by

$$\begin{aligned} \frac{dq_i}{dm} = {} & -\frac{r_{\mathrm{F}}}{4 h_{\mathrm{F}} S (r_{\mathrm{F}} R_{\mathrm{F},i} - r_{\mathrm{G}} l_{\mathrm{G,min}})} \\ & + \frac{h_{\mathrm{F}}}{m^2} \int_0^{t_{\mathrm{F}}} dz \int_{r - a \tan q_{\max,\,i}}^{r} dr \int_{q\,\min}^{q_{\max,\,i}} dq \, r \cos^{-1}\left(\frac{r^2 - r^2 - a^2 \tan^2 q}{2ar \tan q} \right) \sin q \\ & - \frac{1}{} \int^{r} dr \int^{q_{\max,\,i}\big|_{z=t_{\mathrm{F}}}} dq \, r \cos^{-1}\left(\frac{r^2 - r^2 - a^2 \tan^2 q}{} \right) \quad (t_{\mathrm{F}} < z_{\max,\,i}) \end{aligned}$$

From the third term in this equation it is clear that the limit of dq_i/dm as m approaches zero is unbounded; i.e.,

$$\lim_{m \to 0} \frac{dq_i}{dm} = +\infty,$$

so that the derivative is defined for all $m > 0$.